DEVELOPMENT OF A FLOW CYTOMETRY ASSAY TO STUDY MONKEYPOX VIRUS INFECTION AND IMMUNE RESPONSE REGULATION IN NONHUMAN PRIMATES

by

Nicole Marie Josleyn

Bachelor of Science (Shepherd University) 2003

THESIS

Submitted in partial satisfaction of the requirements

for the degree of

MASTER OF SCIENCE

in

BIOMEDICAL SCIENCE

in the

GRADUATE SCHOOL

of

HOOD COLLEGE

December 2019

Accepted:

Reed Johnson, Ph.D.
Committee Member

Ann Boyd, P .D.
Director, Biomedical Science Program

Jeffrey Rossie, Ph.D.
Committee Member

John M. Dye, Ph.D.
Thesis Adviser

April Boulton, Ph.D.
Dean of the Graduate School

STATEMENT OF USE AND COPYRIGHT WAIVER

I do authorize Hood College to lend this thesis, or reproductions of it, in total or in part, at the request of other institutions or individuals for the purpose of scholarly research.

DEDICATION

"Success is achieved by those who work hard"

This thesis is dedicated to:

My husband, my dear love, Matthew, who has given me a lifetime of love and laughter. A source of consistency and support, Matthew inspired me to keep moving forward, despite difficult circumstances, to write this thesis.

My parents, my role models, Jon and Sharon, who raised me to be who I am today. Through their positive example, mom and dad taught me the value of hard work. Through their unconditional love and support, I pursued this scientific research.

My children, Liam and Jacob, who inspired me to be better every day.

My educators, both early childhood and beyond, who have shaped my mind and fed my scientific curiosity.

My mentors, coaches, and friends, who moved me forward, adding value, to each facet of my life. Through their contributions, I am where I am today. I am ready for this next adventure.

ACKNOWLEDGEMENTS

First, I would like to thank my thesis committee members, Dr. John Dye, Dr. Reed Johnson, and Dr. Jeffrey Rossio. Your scientific feedback has been most valuable and honest, and has helped me improve my scientific research and writing. Thank you for reading my early drafts, and being strong critics. Your comments were helpful to me to elucidate the process of writing. Because of your support, I have learned valuable information that will serve me in my scientific career.

I would like to thank the staff at the United States Army Medical Research Institutes of Infectious Diseases (USAMRIID) for your support and encouragement over the years, especially John Dye, Spencer Stonier, Andrew Herbert, Courie Cohen, Jennifer Brannan, Ana Kuehne, Russell Bakken, Samantha Zak, Ray Ortiz, Laura Prugar, Rebekah James, Cecilia O'Brien, Danielle Dorosky, Shawn Abbasi, Kathleen Huie, Kathleen Dempsey, and Kandis Cogliano.

I would like to thank the staff at the Integrated Research Facility and the NIAID Emerging Viral Pathogens Section for your support and encouragement over the years, especially Reed Johnson, Krisztina Janosko, Melanie Cohen, Haifeng Song, Tengfei Zhang, Peter Jahrling, Daniela Pusl, John Bernbaum, Lauren Keith, Lisa Hensley, Gene Olinger, Mike Holbrook, Rebecca Bernbaum, Katie Hagen, Jamie Pettitt, Marisa St. Claire, Russell Byrum, Jennifer Cann, Louis Huzella, Dan Ragland, David Thomasson, Isis Alexander, Nicholas Oberlander, Julia Michelotti, Catherine Jett, Sylvan McDowell, Erika Zommer, Jennifer Sword, Yu (Lucy) Cong, and Steven Mazur.

I would like to thank my science professors at the Hood College Graduate School for your support and encouragement, especially Dr. Ann Boyd, Dr. Jeffrey Rossio, Dr. Ricky Hirschhorn, Dr. Rachel Bagni, and Dr. Craig Laufer.

Funding Disclosure: This work was supported by NIH NIAID DIR and NIH NIAID DCR and funded, in part, through Battelle Memorial Institute's prime contract with the US National Institute of Allergy and Infectious Diseases (NIAID) under Contract no. HHSN272200200016I.

Opinions, interpretations, conclusions, and recommendations are those of the author and are not necessarily endorsed by any branch of the U.S. government.

TABLE OF CONTENTS

ABSTRACT

Monkeypox virus (MPXV) is divided into two clades, Congo Basin and West African. Congo Basin MPXV infection is associated with severe symptoms and fatality of up to 10 percent in humans; whereas, West African MPXV infection is associated with less severe symptoms. To study infection and differential immune response regulation among virus isolates from Congo Basin and West African clades in nonhuman primates, a flow cytometry assay was developed. Annexin V, a protein used to detect apoptosis previously did not permit fixation and permeabilization for intracellular measurements, such as pathogen-infected cells. The method developed permits measurements of Annexin V apoptosis combined with intracellular staining. Reagents compatible with Annexin V were identified for fixation/permeabilization, and the need for calcium in intracellular assay steps was determined. The combined Annexin V/intracellular method described can be used to study disease pathogenesis of many BSL-3 or BSL-4 pathogens in nonhuman primates.

LIST OF TABLES

LIST OF FIGURES

LIST OF ABBREVIATIONS

%	percent
AVBB	Annexin V binding buffer
ATP	adenosine triphosphate
B cells	B lymphocytes
BCR	B cell receptor
BSL-2	Biosafety Level 2
BSL-3	Biosafety Level 3
°C	degrees Celsius
Caspases	cysteine-aspartic acid-specific proteases
CD	Cluster of differentiation
CD4+ T-cells	CD4+ T-lymphocytes
CDC	Centers for Disease Control
CDV	Cidofovir
CO_2	carbon dioxide
CPXV	Cowpox virus
CTLs	cytotoxic T-lymphocytes
DAMP	damage-associated molecular pattern
DCs	dendritic cells
DNA	deoxyribonucleic acid
DRC	Democratic Republic of Congo
FBS	fetal bovine serum
FDA	Food and Drug Administration

FSC-A	forward-scatter area
HEPES	4-(2-hydroxyethyl)-1-piperazineethanesulfonic acid
IFNα/β	IFN alpha/beta
IFNγ	interferon gamma
IgG kappa	immunoglobulin G kappa
kg	kilogram
mg	millogram
MHC	Major Histocompatibility Class
MHC-I	Major-Histocompatibility Complex Class-I
MHC-II	Major-Histocompatibility Complex Class-II
mL	milliliter
MPXV	Monkeypox virus
MVA	modified virus Ankara vaccine
NEAA	non-essential amino acids
ng	nanograms
NK cells	natural killer cells
NIH CC	National Institutes of Health Clinical Center
OPV	Orthopoxvirus
PAMPs	pathogen-associated molecular patterns
PARP	poly(ADP-ribose) polymerase
PBMCs	peripheral blood mononuclear cells
PFU	plaque forming units
p.i.	post-infection

PI	propidium iodide
PMA	phorbol 12-myristate 13-acetate
PRRs	pattern recognition receptors
PS	phosphatidylserine
T-cells	T-lymphocytes
TNFα	tumor necrosis factor alpha
µL	microliters
µM	micromolar
VACV	Vaccinia virus
VARV	Variola virus
ViD	viability dye
VPs	viral proteins
WHO	World Health Organization

INTRODUCTION

Human monkeypox has become a global health security concern. More cases were reported over a wider geographical area in the past decade than over the previous 40 years (Durski *et al.* 2018). Human monkeypox primarily occurs in Central Africa in countries including Central African Republic, Democratic Republic of Congo, Cameroon, Gabon, and Nigeria. Since 2003, the disease has spread into other regions across Africa as well as to continents such as North America and Europe. The most vulnerable population is children under the age of 15, who make up 90 percent (%) of those infected (Jezek *et al.* 1987), and the mortality rate in children under age 10 is about 13% (Arita *et al.* 1985). Many countries lack expertise to detect cases, treat patients, and prevent transmission of this disease. In 2017, a meeting was held in Geneva, Switzerland and attended by members of World Health Organization (WHO), Centers for Disease Control (CDC, Atlanta, Georgia), State Research Center of Virology and Biotechnology VECTOR (Russian Federation), Robert Koch-Institute (Berlin, Germany), and other important stakeholders. Meeting attendees identified the need for improvements in surveillance and response efforts to prevent further geographical spread of human monkeypox (Durski *et al.* 2018). They also identified a need for animal studies to understand differences among viral strains of monkeypox and to rapidly evaluate existing possible countermeasures (Durski *et al.* 2018).

Human monkeypox is caused by Monkeypox virus (MPXV). Monkeypox virus is a member of the genus Orthopoxvirus (OPV) in the subfamily of Chordopoxvirinae, in the family of Poxviridae. The Poxviridae family contains four subfamilies: Molluscipoxviruses, Orthopoxviruses, Parapoxviruses, and Yatapoxviruses. The largest

threat to humans, are viruses of the OPV genera: MPXV, Cowpox virus (CPXV), Vaccinia virus (VACV), and Variola virus (VARV). Additional members of the OPV genus are Camelpox, Cowpox, Ectromelia, Racoonpox, and Taterapox viruses and Uasin Gishu disease (Table 1). Today, the greatest natural threat among OPVs is human monkeypox which has an overall mortality rate of up to 10% (WHO 2018).

Table 1. *Orthopoxvirus* species.

Species	***Animals displaying signs of infection***	***Geographical range***
Camelpox	Camels	Africa, Asia
Cowpox	Cow, man, rats, cats, gerbils, large felines, elephants, rhinoceroses, okapis	Europe
Ectromelia	Mice	Europe
Monkeypox	Monkeys, great apes, anteaters, squirrels, man	Africa, western and central
Racoonpox	Raccoons	USA
Taterapox	*Tatera kempl* gerbil	Africa, western
Uasin Gishu disease	Horses	Africa, eastern
Vaccinia	Man, cow, buffalo, pig, rabbit	World-wide
Variola	Man	Formerly world-wide (now eradicated)

Adapted from Fenner 1988

Poxviridae family members have a characteristic brick-shaped structure, with a large, double-stranded deoxyribonucleic acid (DNA) genome within a viral envelope (Moss and Shisler 2001). Poxvirus genomes are linear and vary in size from 145 to 290 kilobase pairs (Cann 2012). Generally, poxviradae family members have conserved regions located in the center and terminal regions of the genome (Cann 2012) (Figure 1). The conserved regions in the center of the poxvirus genome are dedicated to viral replication and assembly (Cann 2012; Seet *et al.* 2003), while genes in non-conserved regions influence species specificity, pathogenesis, and immunomodulatory properties (McFadden 2005; Moss 2001; Seet *et al.* 2003). In contrast to other DNA viruses,

poxviruses have evolved to rely minimally on the host cell. For example, polyomaviruses and papillomaviruses replicate in the nucleus; however, poxviruses are unique, because they replicate and assemble in the host cell cytoplasm using minimal host cell machinery (Cann 2012).

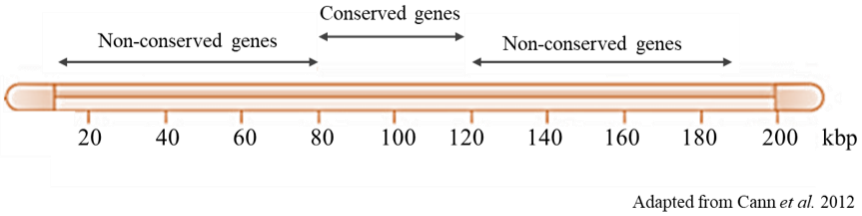

Figure 1. Organization of *Orthopoxvirus* genomes. The outer regions of poxvirus genomes are variable, while the central region tends to be conserved. *Orthopoxvirus* genomes vary in size from 145 to 290 kilobase pairs, with the outer, non-conserved regions influencing species specificity, pathogenicity, and immunomodulatory properties of the virus. The conserved regions are essential to virus replication. The genomic map was available Principles of Molecular Virology (Cann 2012) at https://www.researchgate.net/profile/Akila_Wijerathna_Yapa2/post/Which_is_the_best_book_to_study_molecular_virology/attachment/59d6207c79197b807797ef1d/AS%3A273680301527040%401442261876240/download/Alan_J._Cann_Principles_of_Molecular_Virology.PDF). The figure was adapted to reflect conserved and non-conserved genomic regions.

Monkeypox virus was first isolated from pustular lesions of monkeys during an outbreak in 1958 among a nonhuman primate colony at Statens Serum Institut in Denmark (Magnus *et al.* 1959). The licensed vaccine used during the vaccination program to eradicate global smallpox elicited cross-protection to human monkeypox (Hooper *et al.* 2004; McConnell *et al.* 1964). Cessation of the smallpox vaccination program coincided with emergence of human monkeypox cases in Central Africa, in the Democratic Republic of Congo (DRC) (Huhn *et al.*. 2005; Marennikova *et al.* 1972). Between 1970 and 1979, there were 47 cases of human monkeypox in Africa, and 38 of these cases were localized to the DRC (Breman *et al.* 1980). More cases emerged in the 1980s (Arita *et al.* 1985) and 1990s (Hutin *et al.* 2001), and MPXV eventually made its way to the United States in 2003

(Centers for Disease Control and Prevention 2003). In April 2003, African rodents, including Gambian pouched rats, a suspected reservoir of MPXV (Falendysz *et al.* 2015; Hutson *et al.* 2015; Reed *et al.* 2004), were imported to the United States from Ghana. The imported African rodents were housed at an animal distribution facility in Illinois in close proximity to approximately 200 prairie dogs (Centers for Disease Control and Prevention 2003). Humans contacted these prairie dogs and became infected with human monkeypox. In this United States outbreak, 71 cases of human monkeypox were reported to the CDC, and of these, 35 were laboratory-confirmed (Centers for Disease Control and Prevention 2003).

The most recent outbreak of human monkeypox occurred in the country of Nigeria and proceeded from September 2017 through September 2018**.** This outbreak had 115 identified cases and seven deaths (WHO 2018). And in September 2018, two unlinked cases of human monkeypox spilled over into the United Kingdom originating from travelers to Nigeria (European Centre for Disease Prevention and Control 2018).

Monkeypox virus has a broad host range. A large ecological study conducted in Liberia and Nigeria, in 1971, did not recover MPXV from the organs of over 439 specimens, including monkeys, rodents, and other mammals (Arita *et al.* 1985). A separate study in Zaire in 1979, did not recover MPXV from 98 species, including monkeys, squirrels, antelope, rodents, porcupines, and pangolins (Arita *et al.* 1985). In all, 1,500 animals were tested, and OPV antibodies were present in species of birds, rodents, squirrels, antelopes, and monkeys. In two species, MPXV antibodies were identified by radioimmunoassay-absorption (Arita *et al.* 1985). Monkeypox virus primarily infects rodents and occasionally infects monkeys and humans. Serological

testing is recommended for diagnosis of human monkeypox (WHO 1999). Human transmission most likely occurs when humans come into contact with infected animals. Risk of person-to-person transmission is elevated among household contacts compared to transmission rates among non-household members (Breman *et al.* 1980). Based on ecological niche modeling, the environmental conditions most favorable for human monkeypox transmission are found in humid tropical forest areas of West and Central Africa (Levine *et al.* 2007; Nakazawa *et al.* 2013b).

Two clades of MPXV, Congo Basin and West African, have been confirmed by whole genome analysis (Likos *et al.* 2005; Reed *et al.* 2004, Nakazawa *et al.* 2013a). Monkeypox virus clade members are rooted in CPXV Grishak (Figure 2). Monkeypox virus strains, such as Copenhagen_1958, Sierra Leone_1970, Liberia_1970, and USAGhana_2003, West African MPXV isolates, are West African clade members (Figure 2). Some Congo Basin MPXV isolates include Zaire_1979, Sudan_2005, and Zaire_1996) (Nakazawa *et al.* 2013a).

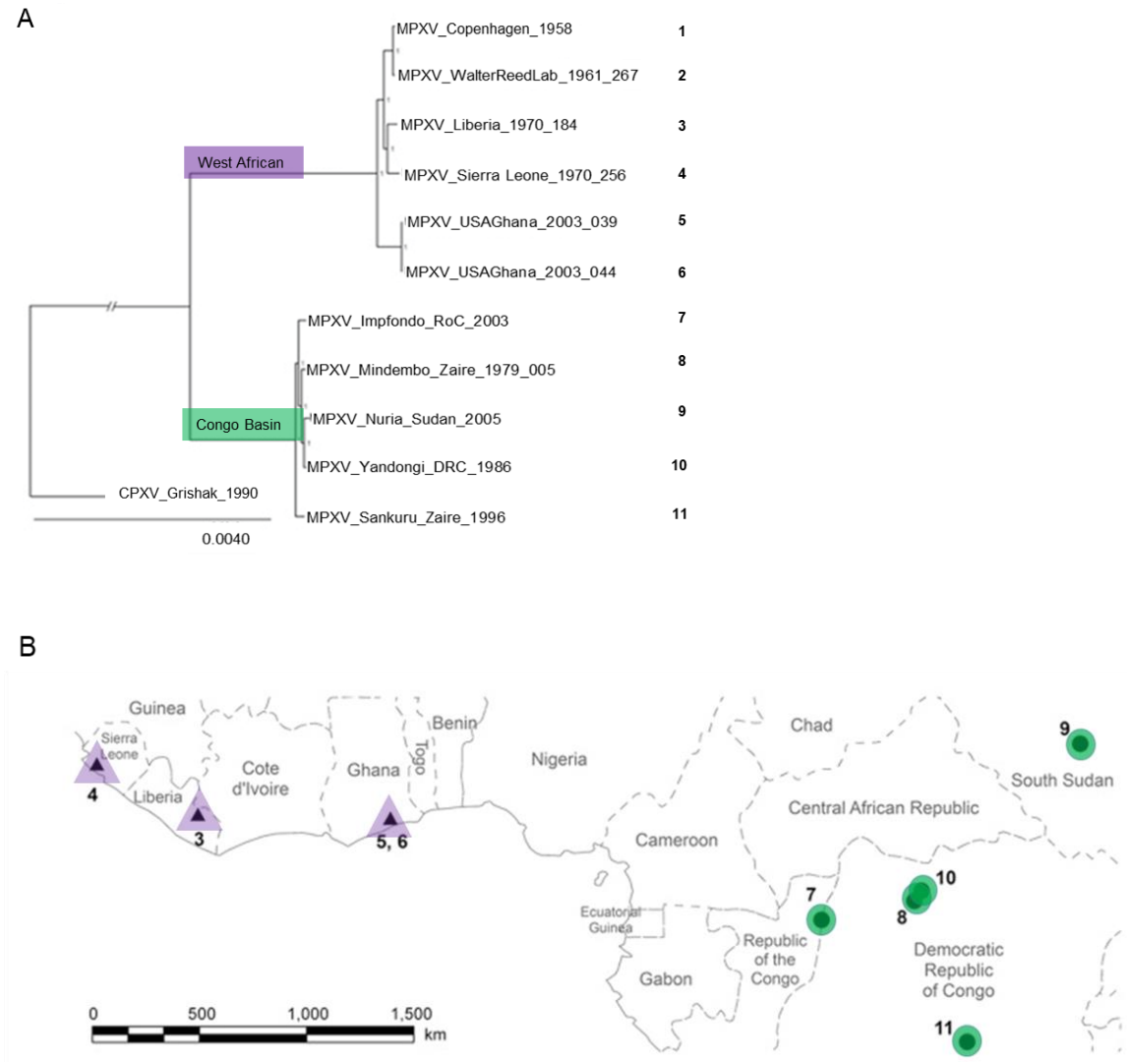

Figure 2. Phylogenetic tree and geographical map of two clades of Monkeypox virus. (A) The phylogenetic tree from 11 Monkeypox virus (MPXV) isolates shows two clades of MPXV, West African (purple) and Congo Basin (green). The scale bar represents the nucleotide substitutions per site. (B) The geographical map of Africa representing the distribution of MPXV among the two clades, West African (purple) and Congo Basin (green). Strains 1 (Copenhagen_1958) and 2 (WalterReed Lab_1961) are not represented on the map because these are laboratory strains. The phylogenetic tree and map were available from Emerging Infectious Diseases (Nakazawa *et al.* 2013a) at (https://www.ncbi.nlm.nih.gov/pmc/articles/PMC3559062/). The figure was adapted to increase text size on the phylogenetic tree to enhance resolution and visibility, and to color-code the clades on the phylogenetic tree and map for ease of recognition.

Monkeypox virus disease has similar clinical presentation as smallpox disease. The disease is characterized by symptoms such as fever, sometimes accompanied by backache, abdominal pain, muscle pain, or headache, and a rash that forms on the skin and within mucous membranes (Nalca *et al.* 2005). The rash progresses through various stages, including papules, vesicles, pustules and umbilicated lesions that result in pitting scars (Breman *et al.* 1980). Lymphadenopathy, or enlarged lymph nodes, is a common feature distinguishing human monkeypox from smallpox. Enlarged lymph nodes are observed in the neck and groin area (Breman *et al.* 1980). Sequelae of human monkeypox include secondary bacterial infections, pulmonary distress, bronchopneumonia, corneal ulcerations, life-long blindness, septicemia and death (Jezek *et al.* 1987). And while the vaccine successfully used to eradicate smallpox shows protective efficacy against monkeypox (Zaucha *et al.* 2001), serious adverse complications exist (Aragon *et al.* 2003; Belongia and Naleway 2003; Cono *et al.* 2003; Poland *et al.* 2005) and vaccination is not recommended for all populations.

Vaccination with the licensed Dryvax vaccine, a live-viral VACV vaccine, has many known adverse side-effects including headache, joint pain, muscle aches, and swollen lymph nodes (Cono *et al.* 2003). The vaccine is known to be life-threatening, causing eczema vaccinatum, progressive vaccinia and encephalitis in immune-compromised individuals (Aragon *et al.* 2003; Cono *et al.* 2003). The vaccine is contraindicated for approximately 15-50% of the US population (Engler *et al.* 2002; Kennedy and Poland 2007) based on previous personal or family history of immunodeficiencies, eczema, psoriasis, atopic dermatitis, cancer, organ transplants, or heart conditions (Cono *et al.* 2003; Kennedy and Poland 2007; Petersen *et al.*. 2015).

Attenuated vaccine strains do exist, but these must be administered in high-doses with repeated boosters in order to provide lasting protective immunity (Earl *et al.* 2004; Jacobs *et al.* 2009; Jahrling *et al.* 2005). At present, the modified virus Ankara (MVA) vaccine strain is in phase I/II clinical trials to assess safety and immunogenicity. Patients with a previous Dryvax-vaccination history will be randomized to receive either one intramuscular injection of 10^8 plaque forming units (PFU) of MVA or placebo, or two injections of MVA or two injections of placebo spaced 4 weeks apart. At twelve weeks, the patients will be challenged with the Dryvax vaccine so immunological responses can be assessed (NIH CC 2008). Vaccines in national stockpiles in the United States include ACAM2000, Imvamune, and Aventis Pasteur Smallpox Vaccine (FDA 2018). Vaccine potencies have been tested using chorioallantoic membrane and rabbit scarification potency assays (Fuller and Kolb 1968). Based on these assay methods, a titer above 10^8 pock-forming units per milliliter was the required specification for vaccine approval. Cell-based assays were developed as a more reliable system to evaluate vaccine potencies among smallpox vaccine lots. Correlation analysis between the various methods indicated that a titer of greater than 7.6 log10 TCID50/ml was expected to generate more than 10^8 pock-forming units per milliliter at the 95% confidence level (Leparc-Goffart *et al.* 2003).

For public health emergencies involving smallpox, there are Food and Drug Administration (FDA) approved therapeutics stockpiled in the United States (CDC 2019). In July 2018, the FDA approved Tecovirimat utilizing the FDA Animal Rule (Grosenbach *et al.* 2018). The FDA animal rule permits animal efficacy data to be used for drug approvals by the FDA when human efficacy trials are not possible. Tecovirimat is an inhibitor of the VP37 protein, a protein conserved among all OPVs that is involved in viral

budding and egress from infected cells (Blasco and Moss 1991; Grosenbach *et al.* 2018; McIntosh and Smith 1996). Tecovirimat has shown greater than 90% protective efficacy at a minimum effective dose of 10 millograms (mg)/kilogram (kg) administered via oral gavage for fourteen days in nonhuman primates intravenously challenged with MPXV, and 40 mg/kg for fourteen days in rabbits challenged intradermally with rabbitpox virus Utrecht (Grosenbach *et al.* 2018). Cidofovir (CDV), a therapeutic approved by the FDA for another indication, has also been approved for smallpox use. Cidofovir, an inhibitor of DNA polymerase, has shown complete protective efficacy in mice exposed to CPXV (Smee *et al.* 2000) or VACV (Smee *et al.* 2001) via intranasal route, and nonhuman primates exposed to MPXV intravenously (Dyall *et al.* 2011; Song *et al.* 2013) or via an intratracheal route (Stittelaar *et al.* 2006). Cidofovir, however, must be administered intravenously (Smee *et al.* 2000, 2003) and in tandem with other therapeutics to reduce renal complications (Bray 2003; Naesens *et al.* 1996; Nalca *et al.* 2005). Recently, modifications to CDV have made oral consumption possible and have led to reduced nephrotoxicity (Foster *et al.* 2017). The modified CDV is called Brincidofovir. Drug-resistance to Brincidofovir is possible; however, since mutations to viruses occur. Weaponization of MPXV could include synthesis of Brincidofovir-resistant properties or other properties making the virus more virulent (Durraffour *et al.* 2012).

Human Immune Response to Viral Pathogens

The human body is capable of detecting and responding to foreign invaders, such as viruses. Generally, when a virus gains entry into a mammalian host through mucus membranes or a physical breach in the skin, the host immune system activates to contain

the virus and prevent its spread. A localized inflammatory response recruits cells capable of destroying the virus.

The immune system is comprised of two distinct arms, the innate and the adaptive immune systems. The early innate immune response provides a first line of defense against invading pathogens within hours of initial pathogen encounter, whereas initiation of the adaptive immune response is delayed, occurring roughly 5 to 6 days following pathogen encounter (Owen *et al.* 2013). Communication between innate and adaptive systems is important for the host to defeat and clear the virus. Cross-talk between these systems occurs through cell-to-cell contact as well as through chemical messages that help guide and direct the adaptive response. The adaptive immune response is required to clear pathogens, resolve infection, and induce immunological memory in the host. Immunological memory allows the host to respond swiftly to fight repeat invaders.

The innate immune system provides a first line of defense when host physical barriers have been breached. Cells of the innate immune system are granulocytes and myeloid cells, including monocytes, macrophages and dendritic cells (DCs). Neutrophils are a subset of granulocytes that are first responders to sites of inflammation. Neutrophils proliferate in the bone marrow and migrate through the blood to the inflammatory site. At the inflammatory site, neutrophils phagocytize pathogens and secrete additional signaling molecules aiding in the recruitment of monocytes and DCs from the blood and bone marrow. Recruited monocytes differentiate into activated macrophages or DCs at the inflammatory site dependent on the signals received.

The viral recognition process is facilitated by pattern recognition receptors (PRR) that are present on immune cells. Pattern recognition receptors bind to pathogen-associated

molecular patterns (PAMPs) on the surface of invading pathogens, such as carbohydrate moieties, cell wall components, or lipid components (Owen *et al.* 2013). When specific PAMPs are encountered by PRRs, innate immune cells respond by engulfing the virus by phagocytosis.

Macrophages are cells involved in phagocytosis and cleanup of aged, damaged, or dying cells. Macrophages are attracted to lysophosphatidic acid that is released from the lipid membrane of cells undergoing programmed cell death at the end of their lifespan or as a result of damage or viral infection (Owen *et al.* 2013). Early apoptosis results in presentation of an 'eat-me' signal expressed on the cell surface that is not present on normal, healthy cells. The 'eat-me' signal occurs via translocation of the protein phosphatidylserine (PS), normally confined to the inner leaflet of the cell membrane, to the outer leaflet of the membrane (Martin *et al.* 1995). Macrophages are particularly adept at sensing PS that localizes on the apoptotic cell surface. Phosphatidylserine expression is a damage-associated molecular pattern (DAMP) resulting in clearance of aged, infected, or damaged cells by macrophages.

When PAMP and DAMP signals are detected at the inflammatory site, activated cells release chemical signaling molecules into the local environment. Released chemical signaling molecules, cytokines and chemokines, drive the host immune response to invading pathogens. Growth cytokines, such as granulocyte colony stimulating factor (G-CSF), reach the bone marrow and serve as signals for the growth and release of more cells to the periphery to fight foreign invaders. Proinflammatory cytokines play an important role in inducing activation and proliferation of immune cells. Chemokines act as chemoattractants to recruit important effector cells to inflammatory sites. Some viruses

have evolved mechanisms inhibiting cytokine transcription that may result in serious or deadly outcomes for the host. In addition to blocking the production of chemical messages, some viruses interfere with release and trafficking of cytokines by encoding viral proteins (VPs) that act as cytokine receptor decoys. Viral proteins that act as receptor decoys prevent important key messages from reaching intended destinations and could inhibit the acute phase immune response to the detriment of the host.

Macrophages and DCs function as the bridge between the host's innate and adaptive immune system. Macrophages and DCs are also called antigen presenting cells, because they engulf pathogens and process them into short stretches of amino acid fragments called peptides. Viral peptides are loaded onto Major Histocompatibility Class (MHC) molecules and transported to the cell surface to alert the host to the presence of foreign invaders through the activation of T-lymphocytes (T-cells). Ineffective presentation of peptides by macrophages and DCs to T-cells can result in failure to activate the adaptive immune system in acute infection and may result in prolonged viral replication and death of the host.

Antigen presenting macrophages and DCs migrate from the inflammatory site via afferent lymphatics to draining lymph nodes. Draining lymph nodes and the spleen are examples of secondary lymphoid organs. The host resourcefully concentrates viruses and immune cell populations into distinct regions of secondary lymphoid organs (Paul *et al.* 2013). Pathogens drained from the blood are collected in the spleen, and pathogens from tissues are drained into local lymph nodes (Paul *et al.* 2013). Tissue resident cells are abundant within specific zones of secondary lymphoid organs to survey these tissues for the presence of pathogens. Macrophages, abundant within red pulp of the spleen, detect

pathogens drained into this zone from the afferent splenic artery. Lymphoid cells from the white pulp, migrate into the red pulp in response to a pathogen, to initiate an adaptive immune response (Paul *et al.* 2013). Extracellular pathogen recognition is mediated by tissue resident cells, neutrophils, macrophages and DCs, but the host's immune system must also recognize and deal with pathogens located within cells, hidden in an intracellular environment.

During a primary infection, one in which the host is encountering a viral pathogen for the first time, natural killer cells (NK cells) are the initial responders to intracellular pathogens. Natural killer cells are innate lymphoid cells originating in the bone marrow. Activated NK cells lack viral-antigen specificity, but they exert a direct killing effect when cells are encountered that have lost Major-Histocompatibility Complex Class-I (MHC-I) on the cell surface. The direct killing effect of infected cells, but not activated NK cells, is mediated by perforin proteins and the release of granzyme proteins (Figure 3). Perforin proteins create pores in the cellular membrane of infected cells. Then granzyme proteins are delivered into infected cells and activate multiple apoptotic pathways. Sacrificing infected cells through programmed cell death is a tactic the immune system employs to clear pathogen infected cells. Viral-mediated inhibition of granzymes and down-regulation of MHC-I would be expected to increase longevity of infected cells. This cellular hijacking by viral pathogens enables the virus to replicate itself inside the host's cells without alerting the host's immune system. Thankfully, the host has additional immune cells, T-cells, with antigen-specificity capable of responding to cellular hijackers.

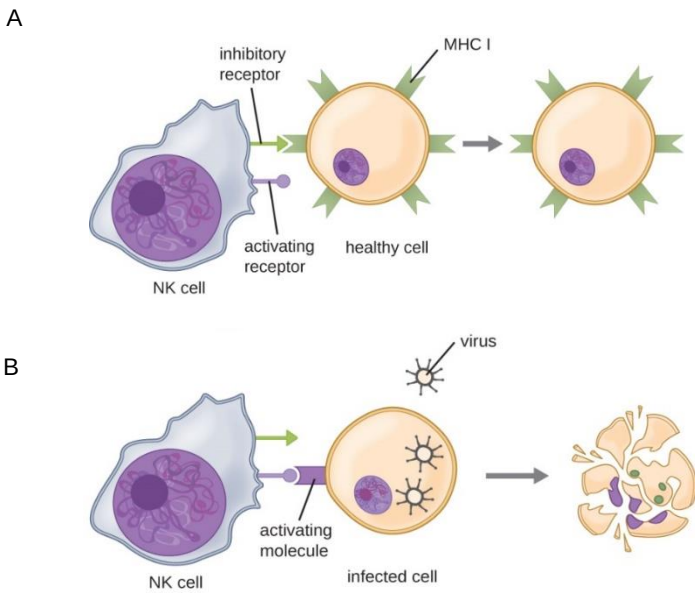

Figure 3. Natural killer cells mediate killing of infected cell by release of perforins and granzymes. (A) Healthy cells are not killed by natural killer cells (NK cells), because they have inhibitory Major Histocompatibility Class I receptors on their surface. (B) Virus infected cells downregulate the inhibitory receptor and express activating molecules on the surface that are targeted by NK cells. Activated NK cells release perforins and granzymes that target infected cells to undergo apoptosis. Picture obtained from OpenStax CNX from Section 17.3 Cellular Defenses, Figure 17.16 (http://cnx.org/contents/e42bd376-624b-4c0f-972f-e0c57998e765@4.2) [accessed 06 October 2019] License CC BY (Creative Commons Attribution License v4.0) (Parker *et al.* 2016).

T-lymphocytes are cells of the adaptive immune system capable of developing antigen-specificity to foreign pathogens. The adaptive immune system is comprised of cellular-mediated immunity and humoral-mediated immunity. T-lymphocytes are components of cellular-mediated immunity. Cellular immunity to viral pathogens is composed of various cellular stages such as resting, activation, proliferation, contraction, and memory phases (Figure 4). T-lymphocytes develop in the bone marrow and migrate to the thymus to undergo differentiation. Once differentiated and educated to self-proteins, T-cells circulate in a naïve or resting state in the blood, spleen and lymph nodes. Cells can be classified according to the cluster of differentiation (CD) markers expressed on the cell's

surface. T-lymphocytes are CD3+ and differentiate mainly into CD4+ and CD8+ subsets. Activation of CD8+ cytotoxic T-lymphocytes (CTLs) and CD4+ T-cells is governed by recognition of antigenic peptide fragments through the T-cell Receptor complex and co-engagement of CD28 receptor on the T-cell surface. CD4+ T-lymphocytes recognize antigen presented through MHC Class II molecules (MHC-II), and CTLs recognize antigen presented through MHC-I molecules. These CTLs and CD4+ T-cells undergo a massive expansion phase mediated by secreted cytokines to generate an army of antigen-specific cells. Immune-mediated cellular recognition and killing of infected cells is mediated by CTLs; however, these cells have a delayed response of 7 to 10 days before they proliferate, differentiate, and obtain their antigen-specificity (Paul *et al.* 2013). The expanded population of CTLs leave the lymph nodes and receive signals to perform their various functions at sites of infection. Similar to NKs, CTLs release granzyme proteins that act directly on infected cells to induce apoptosis through delivery of destructive perforin and granzymes to cells presenting viral antigen (Paul *et al.* 2013). CD4+ T-lymphocytes are called helper T-lymphocytes, because they provide necessary secondary signals that enable immune cells to activate and respond to pathogens.

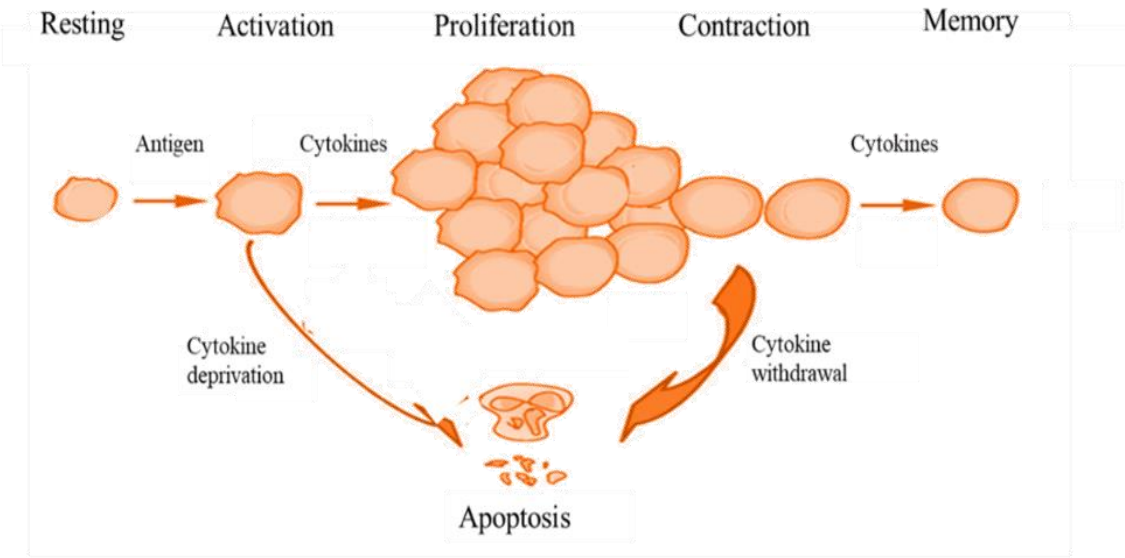

Figure 4. Cellular immune response of CD8+ T-cells to antigen stimulation. Resting CD8+ T-cells are activated by antigen, but in the absence of specific cytokine signaling molecules, activated CD8+ T-cells undergo apoptosis. Activated CD8+ T-cells (cytotoxic lymphocytes; CTLs) proliferate, in the presence of cytokine signals, to create an expanded population of antigen-specific CTLs. At the conclusion of the immune response, cytokine signals drive some CD8+ T-cells toward a memory phenotype, while other CD8+ T-cells undergo contraction through cytokine withdrawal and apoptosis. The figure was adapted with permission from Michael Lenardo, NIAID/NIH (https://www.niaid.nih.gov/research/michael-j-lenardo-md), and simplified by removing cytokine names and the Treg cell population (Lenardo 2017). Courtesy: National Institute of Allergy and Infectious Diseases.

B lymphocytes, originating in the bone marrow (B cells), and the antibodies they produce make up the humoral components of the adaptive immune system. B cells are derived in the bone marrow and migrate into the secondary lymphoid organs, including the lymph nodes and the spleen. B cells have a B cell receptor (BCR). When the BCR is engaged, a process known as cross-linking, the immature B cell undergoes apoptosis. Alternatively, a mature B cell that has an engaged BCR undergoes proliferation. This process, creates a clonal population of B-cells capable of differentiating into plasma cells which are antibody-secreting factories. The antibodies these terminally-differentiated plasma cells secrete are specific and have high affinity for the inducing antigen. Antibodies secreted by plasma cells have important effector functions, such as neutralizing virus,

opsonizing pathogens, fixing complement to enhance phagocytosis or directly lysing pathogens, or inducing NK cells to initiate antibody-dependent cell-mediated cytotoxicity. A portion of the activated, mature B cells, differentiate into long-lived memory cells. Deregulation in BCR cross-linking could result in a hyperactive response, B cell tumors, and autoimmune diseases (Paul *et al.* 2013). Therefore, the process of BCR signaling is tightly regulated.

Two signals are required for mature B cells to proliferate and differentiate into antibody-secreting B cells (Owen *et al.* 2013). First, mature B cells may be activated directly through antigen cross-linking of the BCR. Second, a required signal from activated CD4+ T-lymphocytes (CD4+ T-cells) to mature B cells is needed to induce proliferation and differentiation of B cells into plasma cells or memory cells. In less common instances, B cells may receive information from innate immune cells, such as antigen presented by DCs or macrophages, and become activated. An exception to this two-signal mechanism exists for memory B cells, which require only one signal to engage in a recall response. One signal, in contrast to two, allows the host to swiftly respond to previously encountered pathogens.

Following the activation and proliferation phases is the contraction phase. During the contraction phase, programmed cell death occurs to reduce the numbers of clonally-expanded antigen-specific cells and return the host's immune system to homeostasis. The end of the immune response occurs from cytokine withdrawal, apoptosis, and clearance of apoptotic debris (Figure 4).

Cell Death Pathways Regulated by Pathogens

Programmed cell death, or apoptosis, is the orderly self-destruction of cells that does not trigger a broad host inflammatory response. Caspases are the main proteins activated in apoptosis. Caspases, or cysteine–aspartic acid proteases, are divided into two categories, initiator caspases and executioner caspases. Initiator caspases, such as caspases 2, 8, 9, and 10, undergo cleavage of their pro-domain regions, and the cleaved large and small subunits interact with executioner caspases to induce activation. Executioner caspases are caspases 3, 6, and 7. Activated caspase-3 is the main effector of apoptosis (Slee *et al.* 2001). Activated caspase-3 is responsible for cleavage of many enzymes, including nuclear enzyme poly (ADP- ribose) polymerase (PARP). Poly (ADP-ribose) polymerase is an enzyme involved in repair of DNA strand breaks in the nucleus, and cleavage of PARP is a hallmark of cell death. Apoptosis results in chromatin condensation, DNA fragmentation, cell shrinkage and membrane blebbing (Wlodkowic *et al.* 2012), but the cell membrane remains intact. By antagonizing apoptotic pathways in the host, viruses are able to replicate themselves to higher titers for an extended period of time.

Two pathways converge on executioner caspases, caspases 3, 6, and 7. The extrinsic pathway, described above, is mediated through formation of the death-inducing signaling complex. Signaling at the cell surface mediated through a death receptor (e.g., FasR), leads to oligomerization of procaspase-8 and FADD, to initiate the caspase-cascade (Figure 5). The second pathway, converging on caspase-3, is the intrinsic pathway. The intrinsic pathway, activated by internal cellular stress, results in permeabilization of the outer mitochondrial membrane and cell death (Figure 5). Viruses

frequently target caspases to inhibit apoptosis, since cell death by apoptosis would activate the innate and adaptive immune response.

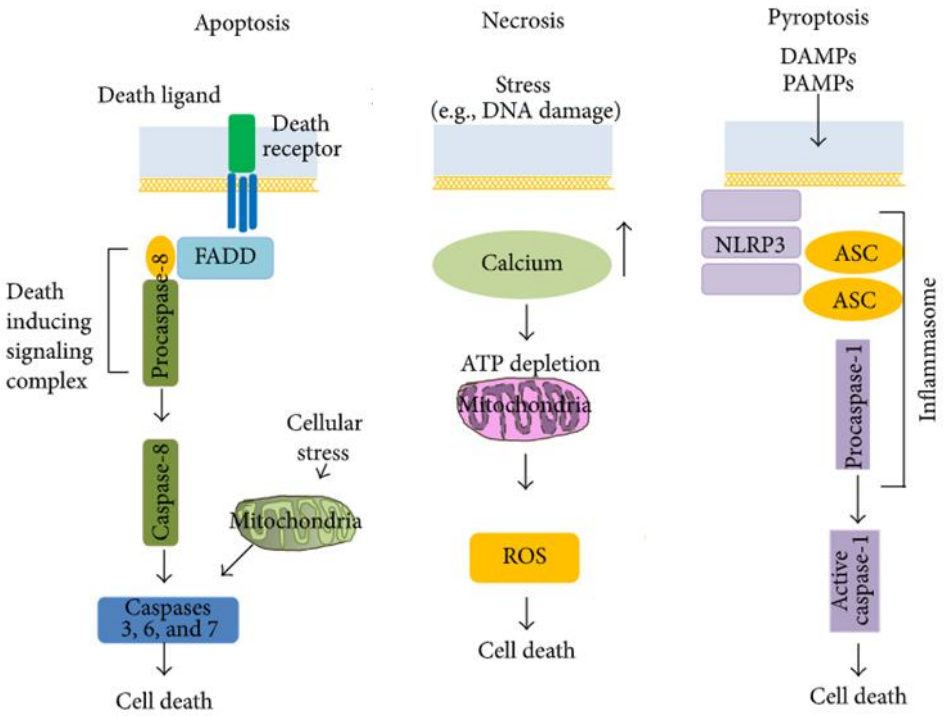

Figure 5. Apoptosis, necrosis, and pyroptosis cell death pathways. Apoptosis, necrosis and pyroptosis pathways are shown. Apoptosis is induced when a death ligand triggers a death receptor, resulting in oligomerization of FADD and procaspase-8 into the Death inducing signaling complex. This complex activates Caspase 8, which further activates executioner caspases 3, 6, and 7, resulting in cell death by apoptosis. The intrinsic apoptosis pathway is initiated by cell stress sensed by the mitochondria, which results in activation of executioner caspases. Necrosis is a cell death pathway caused by stress, such as DNA damage. Elevation of internal calcium results in adenosine triphosphate (ATP) depletion in the mitochondria, and generation of reactive oxygen species (ROS). Necrosis results in cell death with inflammation and release of cellular contents. Pyroptosis is a cell death pathway initiated by DAMPs and PAMPs. Pyroptosis signaling occurs through Caspase-1 and results in inflammation, expulsion of cell contents, and cell death. Picture obtained from Research Gate from Apoptosis, Necrosis, and Necroptosis in the Gut and Intestinal Homeostasis, Figure 2, (Negroni et al. 2015) (https://www.researchgate.net/publication/283674912_Apoptosis_Necrosis_and_Necroptosis_in_the_Gut_and_Intestinal_Homeostasis) [accessed 12 October 2019] License CC BY (Creative Commons Attribution License v3.0). The picture was adapted to reflect only apoptosis, necrosis, and pyroptosis by removal of additional cellular death pathways.

In viral infections, inhibition of apoptosis may lead to necrosis (Upton and Ka-Ming Chan 2014). Necrosis can be caused by DNA damage, changes to intracellular

calcium concentration, increasing amounts of reactive oxygen species, depletion of adenosine triphosphate (ATP), and activation of extrinsic death receptors (Moriwaki and Ka-Ming Chan, 2013; Vanlangenakker *et al.* 2012) (Figure 5). Physiological characteristics of necrosis include changes to organelle structure, swelling of the cell, and loss of integrity of the plasma membrane. Necrosis, in contrast to apoptosis, is a process that results in cell rupture and expulsion of cytoplasmic contents, triggering an inflammatory response in the host (Upton and Ka-Ming Chan 2014). Pathogens employ necrosis strategies to disseminate to new host cells.

Pyroptosis, similar to necrosis, is a cell death pathway that results in cell lysis and extrusion of cellular contents. Pyroptosis is proinflammatory, and triggered by intracellular pathogens. In contrast to necrosis; however, pyroptosis is mediated through caspase 1. Caspase 1 functions to cleave cytokines IL-1B and IL-18 to generate their mature forms, which have protective anti-inflammatory roles in the host cell (Man *et al.* 2018; Fantuzzi and Dinarello 1999). Pathogens that antagonize caspase 1 may do so to replicate and enhance survival in the host cell. Delayed detection by phagocytes, in pyroptosis and necrosis, is an advantage to the pathogen. The pathogen is thereby able to spread prior to being recognized by phagocytes.

Apoptosis, necrosis, and pyroptosis have been implicated in hemorrhagic manifestations of VARV pathogenesis (Wahl-Jensen *et al.* 2011). In Wahl-Jensen et al., cynomolgus macaques were intravenously inoculated with 10^8 or 10^9 PFU of VARV. Poxvirus antigen was detected in the spleen and liver as early as day 1 post-infection (p.i.) by immunohistochemistry. Poxvirus antigen was not detected in lymph nodes from subjects in the 10^8 PFU group, but was by day 3 in the 10^9 PFU group. Viral antigen

staining was observed in the cytoplasm of macrophages. Lymph nodes were enlarged and contained elevated numbers of neutrophils. Apoptotic debris was observed at day 2 p.i. Plasma cells accumulated in the spleen by day 9 p.i. (Wahl-Jensen *et al.* 2011).

The MPXV VPs, F3L, D5R, B19R, B12R and C2L are known to interfere with, or block, apoptosis (Seet *et al.* 2003; Shchelkunov *et al.* 2002). Sequence identities of MPXV Zaire 96 genes encoding F3L, D5R, B19R, B12R, and C2L (NC_003310.1) were analyzed to determine percent identity with homologous regions of the VARV genome (VARV NC_001611.1) (Table 2). The alignments, performed in Blast NCBI, resulted in 100% query coverage with E-values of 0. Sequence identities between MPXV and VARV genomes were 92% or greater, with genes encoding D5R, B12R, and C2L having the highest degree of sequence homology at 97, 96, and 95%, respectively. Genes with a high degree of sequence homology may result in VPs that perform similar functions. Reduced sequence homology resulting from variations in nucleotides among these genes may account for severity and virulence differences among smallpox and monkeypox diseases.

Table 2. Sequence identities among genes encoding MPXV viral proteins that inhibit apoptosis and VARV nucleotide sequences.

MPXV Viral Protein	MPXV Nucleotide Sequence	VARV Nucleotide Sequence	Query Coverage (%)	E-Value	Percent Identity (%)
D5R	9567-10295	3887-4615	100	0.0	97
B12R	170707-171741	161949-162983	100	0.0	96
C2L	26384-27511	18912- 20033	100	0.0	95
B19R	178963-180036	172290-173363	100	0.0	94
F3L	48048-48509	38632-39093	100	0.0	92

Blast NCBI/aligned
VARV GenBank Accession Number NC_001611.1
MPXV Zaire 96 GenBank Accession NC_003310.1

Host survival to OPV infection is dependent upon a successful primary immune response, programmed cell death, viral clearance, and return to homeostasis for the host. To gain more insight into immune components required for viral clearance and host survival, Fang and Sigal performed experiments with CD40-deficient mice (Kawabe *et al.* 1994), CD154-deficient mice (Renshaw *et al.* 1994), CD8-deficient mice (Fung-Leung *et al.* 1991), B-cell-deficient mice (Kitamura *et al.* 1991) and immunocompetent C57BL/6 mice exposed to ECTV (Fang and Sigal 2005). Fang and Sigal showed an important role for CTLs early in ECTV infection. CD8-deficient mice succumbed to ECTV infection within 8 and 10 days and had significantly higher viral loads in the spleen compared to immunocompetent mice or CD40-deficient mice. Fang and Sigal also showed an important role for B cells later in infection for viral clearance. CD40 receptors on the B cell surface interact with CD154 receptors on CD4+ T-cells to mediate antibody production (Noelle *et al.* 1992; Banchereau *et al.* 1994). Fang and Sigal showed CD40-deficient mice controlled viral titers in the spleen early in infection, but the virus disseminated to multiple tissues later in infection, including the liver, lung, tail and ear. CD40-deficient mice succumbed to ECTV within 20 to 70 days p.i., whereas C57BL/6 mice were protected from ECTV (100% survival) (Fang and Sigal 2005). CD154-deficient mice had a similar time to death upon ECTV infection as CD40-deficient mice. Survival of CD57BL/6 mice was attributed to the effectiveness of both the innate and adaptive immune response, as opposed to the inability of the virus to replicate (Karupiah *et al.* 1996). In B-cell deficient mice, virus replication persisted at low levels for a sustained period of time. B-cell deficient mice had a delayed time to death of up to 90 days (Range 25-90 days) (Fang and Sigal 2005). Together, these data showed an important role for B cells and antibody production in viral

clearance and host survival. Furthermore, these data suggested the mere presence of CTLs, in the absence of B cells, was not sufficient to clear virus.

In a separate study by the same authors, NK cells were studied in ECTV infection and were found to have an early and important role controlling viral dissemination to tissues (Fang *et al.* 2008). Virus levels in the spleens and livers of NK cell-depleted C57BL/6 mice (anti-NK1.1 monoclonal antibody PK136-treated) were 10^3-fold higher at day 7 p.i. compared to immunocompetent mice. In immunocompetent mice, by 48 hours p.i., NK cells had migrated into the draining lymph node and cell numbers increased two- to four-fold. Cytokine and granzyme secretion was detected 24 hours p.i. and peaked at 48-hours p.i. In contrast, in the spleen and non-draining lymph nodes, NK cell functional responses were not detected until 5 days p.i. The authors showed that NK cells of immunocompetent mice controlled virus dissemination during early infection by migrating to and acting within the draining lymph nodes. Similar studies depleting cell populations and studying virus-host interactions in MPXV have not been reported.

Monkeypox virus Zaire 96 genes encoding F3L, D5R, B19R, B12R, and VPs were aligned with homologous regions of the ECTV genome (ECTV NC_004105.1) (Table 3). The alignments in Blast NCBI resulted in 100% query coverage with E-values of 0. Alignment of MPXV genes with ECTV nucleotide sequences yielded 91% or greater sequence homologies among all genes queried. Genes encoding D5R and B19R had the greatest degree of sequence homologies, at 98, and 95%, respectively.

Table 3. Sequence identities among genes encoding MPXV viral proteins that inhibit apoptosis and ECTV nucleotide sequences.

MPXV Viral Protein	MPXV Nucleotide Sequence	ECTV Nucleotide Sequence	Query Coverage (%)	E-Value	Percent Identity (%)
D5R	9567-10295	19658-20383	100	0.0	98
B19R	178963-180036	193499-194572	100	0.0	95
B12R	170707-171741	182164-183198	100	0.0	94
C2L	26384-27511	34170-35291	100	0.0	94
F3L	48048-48509	56526.-57098	100	0.0	91

Blast NCBI/aligned
MPXV Zaire 96 GenBank Accession Number NC_003310.1
ECTV GenBank Accession Number NC_004105.1

Monkeypox virus Copenhagen – B19R encodes IFN alpha/beta (IFNα/β binding proteins that bind type I IFNα/β receptors and prevent pathway signaling (Colamonici 1995). Binding to IFNα/β receptors is expected to disrupt early anti-viral signaling in the host cell and result in enhanced virulence. Attenuation of ECTV in mice resulted from deletion of the ECTV – B19R gene (Xu *et al.* 2008). Spleen and draining lymph nodes sizes were reduced and necrotic tissues were not observed, in comparison to mice receiving wild type ECTV (Xu *et al.* 2008). Moving forward, determining contributions of MPXV genes that enhance virulence in non-human primates will greatly aid in development of targeted therapeutic strategies and safer vaccines.

Epidemiological data has been used to compare two clades of MPXV, West African, and Congo Basin (Esposito and Fenner 2001, Likos *et al.* 2005). Human data generated from outbreaks in Africa from 1981–1986 showed more severe symptoms among the MPXV Congo Basin clade compared to the MPXV West African clade (Likos

et al. 2005). Overall, the mortality rate of MPXV Congo Basin was up to 10% (WHO 2018). From 1981 to 1986, there were no fatal cases of MPXV West African. Also, among 71 human MPXV West African cases in the United States in 2003, there were no fatalities (Centers for Disease Control and Prevention 2003).

Studies among nonhuman primates have been performed to understand pathophysiology and virulence differences among MPXV clades (Chen *et al.* 2005; Saijo *et al.* 2009). Results from the Saijo *et al.* indicated the Congo Basin representative strain, Zr-599, replicated in more tissue systems, and resulted in more severe pathological findings relative to MPXV West African (Saijo *et al.* 2009). In addition, the viral genome levels in the blood were10 times higher in non-human primates infected with Zr-599 compared to Liberia strain (Saijo *et al.* 2009).

Although investigations into virulence, genomic differences and pathophysiology differences have been informative, we sought to study infection and differential immune response regulation among nonhuman primates challenged with Zaire 79 or Sierra Leone, representative of MPXV Congo Basin and MPXV West African, respectively. To study immunopathogenesis in peripheral blood, lymph nodes, and spleen of nonhuman primates, a flow cytometry assay was developed.

Introduction to Flow Cytometry

Flow cytometry is a popular scientific technique used to measure physical and chemical characteristics of cells. In flow cytometry assays, cells are labeled with proteins or antibodies that can be measured by an instrument called a flow cytometer. Flow cytometry is used to diagnose diseases, such as primary immunodeficiency diseases (Kanegane *et al.* 2017), and cancers, such as leukemia (Weir and Borowitz 2002; Krause *et al.* 1988) and lymphoma (Barlogie *et al.* 1980). Most commonly, flow cytometry is used

for immunophenotyping, a process of labeling cells for identification for studying the immune response. For example, a CD3 antibody can be used to immunophenotype CD3+ T-cells based on the CD3 antigenic receptor on the cellular surface. Flow cytometry can also be used to identify virus-specific RNA inside cells (Borzi *et al.* 1996), or to detect DNA content for proliferation studies or cell cycle analysis. Flow cytometry is also useful for specific-identification of cells in varying stages of apoptosis, and for labelling dead cells that have a non-intact, compromised cell membrane.

The flow cytometer is composed of three main components, the electronics, the optics, and the fluidics. Samples are first loaded at the sample injection port of the flow cytometer, where the cells travel in a fluidics stream to the flow cell. At the flow cell, cells are hydro-dynamically focused as they pass through laser beams for interrogation (Figure 6). The lasers emit light that travels through fiber optic cables and lenses, or prisms. Fiber optic cables, or prisms direct the light to the flow cell. The emitted laser light makes contact with the cells, and excites fluorochromes on antibodies and proteins for analysis. The forward-scattering properties of light on the blue laser line (488nm) are useful in determining cell size. Cell granularity is measured from side-scattering properties of light (Figure 6). Fluorescent measurements are made based on side-scatter properties of fluorochrome-emitted light. Photons are sent to photomultiplier tubes or photodiodes, where the photons are amplified and converted to an electrical current that becomes a digital value.

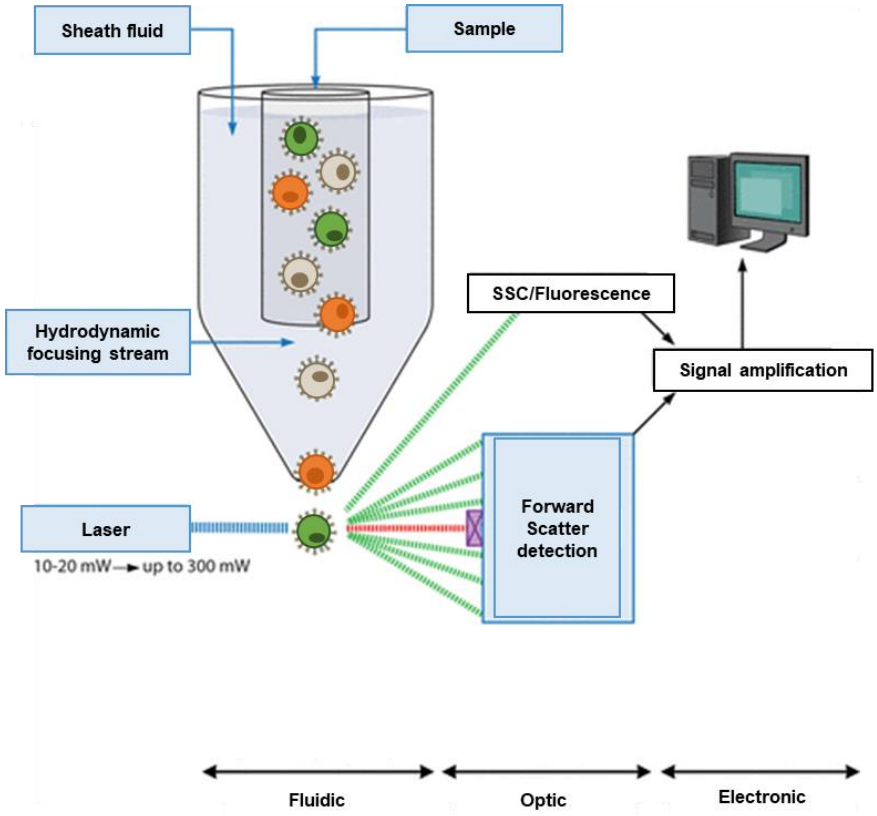

Figure 6. Schematic of fluidics, optics, and electrical components of a flow cytometer. Sheath fluid and cells travel through the core of a flow cell, where the fluidics stream is narrowed to influence cells to move one-at-a-time through the laser beam for interrogation. Emitted light is scattered in the forward direction (forward scattering) and in the side direction (side scattering, SSC/Fluorescence). The scattered light is amplified and converted into a digital value that is stored on a computer. Properties such as cell size and granularity can be measured based on scattering of light in the forward and side directions, respectively. Picture available from http://jvi.asm.org/content/92/3/e01765-17/figures-only?sid=78bb846b-51d8-4280-905e-f4232489c287 Figure 1 [accessed 17 October 2019] (Lippé 2018) Reproduced with permission from the American Society of Microbiology. This figure was adapted by adding cells and enhancing the resolution of the text.

Numerous sample types can be analyzed in a flow cytometer, including sera, plasma, whole blood, peripheral blood mononuclear cells, spleen cells, and bone marrow aspirate. Tissue samples must first be processed to single-cell suspensions and passed through a mesh or nylon filter to remove clumps, prior to flow cytometry. To process some tissues to a single cell suspension, enzymes are used to break down connective tissues in

organs, such as liver, heart, or the lungs, such that cellular populations within these tissues can be released for analysis.

Antibody cocktails, or staining mixes, are used to label specific cellular populations. Protein conjugates covalently attached to antibodies are called fluorophores or fluorochromes. Multiple fluorochromes are attached to a single antibody or protein. The greater the fluorochrome/protein (F/P) ratio, the brighter the light is that is emitted upon excitation of these molecules. Complex analyses of samples can be performed, using an array of antibodies conjugated to different fluorochromes, each with unique fluorescent excitation and emission properties.

Studying MPXV Viral Infection, Proliferation, and Cell Death by Flow Cytometry

Flow cytometry is a useful tool to study immune cell subsets, cell activation, proliferation, and cell death in the blood and secondary lymphoid tissues of nonhuman primates during MPXV infection. Methods for studying cell proliferation and cell death have steadily evolved over the past few decades.

Cells in active phases of the cell cycle (e.g., S, G2/M) express the Ki67 protein. The Ki67 protein is commonly used for measuring cellular proliferation. The original Ki67 antibody was limited to flow cytometry (Gerdes *et al.* 1983), since Ki67 could not be detected in formalin-fixed paraffin sections (Scholzen and Gerdes 2000). At present, several Ki67 antibodies are now available (e.g., MIB-1, MIB-5, SP-6, 30-9, poly, B56) (Acs *et al.* 2017), and these antibodies have been used for Ki67 proliferation detection in a variety of species, including mouse, non-human primate and human.

Rabbit anti-VACV Lister antibody can be used to measure MPXV infection. This antibody has been used to study progression of *Orthopoxvirus* infections among nonhuman

primates challenged with CPXV (Johnson *et al.* 2011) and MPXV (Song *et al.* 2013). In Johnson et al., Rabbit anti-VACV Lister was used for virus detection by immunohistochemistry in nonhuman primate tissues (Johnson *et al.* 2011). Song et al. used Rabbit anti-VACV Lister to study disease progression in MPXV and CPXV by flow cytometry, and described the presence of virions in phagocytes, as a correlative predictor of moribund endpoint (Song *et al.* 2013).

During cell death, cell shrinkage can be measured as a decrease in forward-scatter area (FSC-A) using flow cytometry, but this alone is not a reliable indicator of apoptosis (Wlodkowic *et al.* 2012). Apoptotic cells can be more specifically identified through the use of fluorescently-conjugated proteins and antibodies specific for cell death pathway components, such as activated caspases, cleaved PARP, and Annexin V.

Fluorescently-conjugated Annexin V can be used to measure apoptosis induced by MPXV. Annexin V is an anticoagulant protein that preferentially binds PS exposed on apoptotic and necrotic cells in a calcium-dependent manner (Martin *et al.* 1995). In healthy, non-apoptotic cells, PS is confined to the inner leaflet of the plasma bilayer. In apoptosis, PS is translocated to the outer membrane and localized at the exterior cell surface (Figure 7). Membrane PS exposure occurs early in apoptosis, hours before morphological changes are detected (Martin *et al.* 1995). Membrane PS expression occurs in the presence of a variety of cell death-inducing agents, but is not detected when apoptosis pathways, such as the Bcl-2 and Abl pathways, are inhibited (Martin *et al.* 1995).

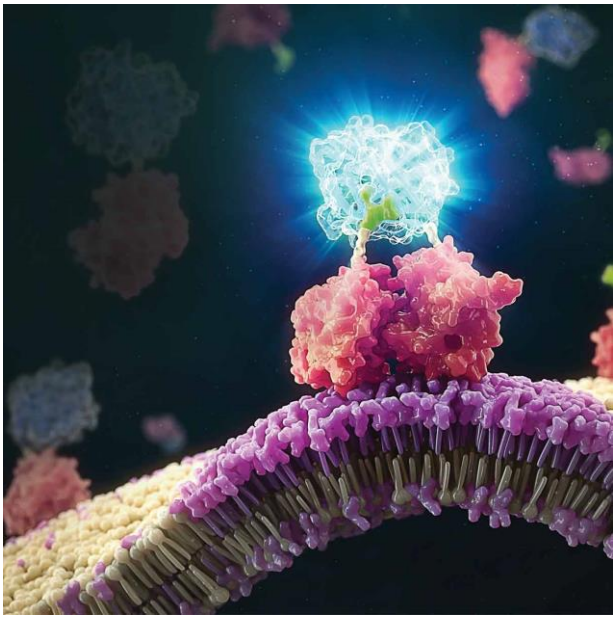

Figure 7. Annexin V detection of translocated phosphatidylserine (PS) by flow cytometry. Phosphatidylserine, normally confined to the inner membrane of the cell, is translocated and localized at the cell surface of cells undergoing cell death (PS, pink color). Annexin V binds PS in a calcium-dependent manner (Annexin V, red color). Annexin V, linked to a fluorochrome conjugates, can be used to quantitate cells undergoing apoptosis by flow cytometry. In this picture, the fluorochrome-conjugated Annexin V molecule is emitting light upon laser excitation by flow cytometry. Picture available at https://promega.media/-/media/images/resources/articles-and-publications/pubhub/featured-articles/annexin-v-feature/annexinv-apoptosis-detection-1200x1200.jpg (Promega Corporation 2019). Reproduced with permission from Promega Corporation. Copyright 2019. All Rights Reserved.

The combination of Annexin V and a vital dye can be used to distinguish early apoptosis from late apoptosis and necrosis. Necrotic cells take up the vital dye, whereas early apoptotic cells do not. Annexin V staining is commonly performed in combination with 7-aminoactinomycin D (7-AAD) or propidium iodide (PI) for analysis of early and late apoptosis by flow cytometry. The use of 7-AAD or PI dyes; however, are not ideal for combined surface and intracellular staining in flow cytometry with Annexin V. Upon long incubations times, PI stains live, intact cells (Wlodkowic *et al.* 2011). Furthermore, samples stained with 7-AAD or PI should not be washed following staining, because these dyes can dissociate from the double-stranded DNA to which they have bound (ThermoFisher 2019). Fixable-amine viability dyes (ViD) (ThermoFisher 2019) are a

better choice for combined surface and intracellular staining in flow cytometry with Annexin V, since these dyes cross compromised cell membranes and bind free-amines in the cytoplasm resulting in their bright fluorescence. Additionally, these dyes are compatible with cellular fixation and permeabilization (ThermoFisher 2019) required to inactivate MPXV prior to data acquisition by flow cytometry at Biosafety Level 2 (BSL-2).

The primary aim of this thesis was to develop a flow cytometry assay to enable scientific investigation of the immune response of rhesus macaques to MPXV infection, to phenotype immune cell subsets containing intracellular MPXV VPs in the blood and secondary lymphoid organs, and to measure clonal expansion and contraction among those cell subsets, through measurements of proliferation, and early apoptosis and necrosis, respectively. The development of an assay is described that enabled combined surface and intracellular staining with Annexin V and fixable-amine viability dyes. Annexin V/PI and Annexin V/7-AAD methods are commonly reported in the scientific literature; however, these methods do not permit combination intracellular staining for flow cytometry. In this thesis, an Annexin V/fixable-amine ViD method was developed to permit Annexin V surface staining in combination with intracellular staining. Fixation and permeabilization reagents were identified and calcium requirements determined that resulted in comparable Annexin V expression to unfixed cells. The role of calcium following fixation and permeabilization, and the stability of Annexin V was studied. Additionally, a mixed population assay was used to study the effect of Annexin V transfer to localized, unoccupied PS sites upon fixation and permeabilization. With minor modifications, this

assay could be adapted to study immunopathogenesis of other infectious diseases that require fixation prior to analysis by flow cytometry.

MATERIALS AND METHODS

Reagents and Materials

The NIH Nonhuman Primate Reagent Resource was reviewed to determine antibody clones cross-reactive to rhesus macaques (NHP Reagent Resource 2004) to be incorporated into a flow cytometry panel. The antibodies and reagents, fluorochromes, vendors, catalog numbers and clone information are shown in Table 4. Labeling cells with Annexin V, Viability Dye (ViD) and monoclonal antibodies was performed in 5-milliliter (mL) tubes in a 100 microliters (µL) final volume. For Annexin V staining, cells were washed twice in 1 mL 1X Annexin V Binding Buffer (AVBB, BD Biosciences, Franklin Lakes, NJ). For experiments requiring phenotyping, the following antibody panels used in a final volume of 100 µL. For experiments requiring intracellular fixation and permeabilization, antibodies were prepared in BD Perm/Wash buffer for staining in a final volume of 100 µL. Monkeypox VPs were detected using an indirect staining procedure with purified Anti-Vaccinia followed by a secondary antibody labeled with Alexa Fluor 750 (Invitrogen Thermo Fisher Scientific, Carlsbad, CA).

Table 4. Summary of antibodies, vendors, catalog numbers, and clone information used for flow cytometry assay development.

Antibody/Probe	Fluorochromes	Target Population	Vendor/Catalog #/Clone
Annexin V	APC	Apoptotic cells (Annexin V+/Fixable-Amine Viability Dye -)	BD Biosciences/550474
Annexin V	FITC	Apoptotic cells (Annexin V+/Fixable-Amine Viability Dye -)	BD Biosciences/556419
CD3	Pacific Blue	T-cells	BD Biosciences/SP34-2
CD4	PE	T-cell subset, CD4+	BD Biosciences/L200
CD4	V450	T-cell subset, CD4+	BD Biosciences/L200
CD8	AmCyan	T-cell subset, CD8+ +	BD Biosciences/SK1
CD8	APC	T-cell subset, CD8+ +	BD Biosciences/SK1
CD11c	APC	Dendritic cell subset, myeloid (CD11c+HLA-DR+)	BD Biosciences/S-HCL-3
CD14	Pacific Blue	Monocytes/macrophages	BD Biosciences/M5E2
CD16	PE	NK cells (CD3-CD16+)	BD Biosciences/3G8
CD20	FITC	B cells	BD Biosciences/L27
CD20	eFluor450	B cells	Biolegend/2H7
CD45	PerCP	Pan-hematopoietic cells	BD Biosciences/D058-1283
CD123	PE	Plasmacytoid dendritic cell subset (HLADR+CD123+CD11c-)	BD Biosciences/7G3
HLA-DR (MHC-II)	V500	Dendritic cells (CD14-HLA-DR+); monocytes/macrophages (CD14+HLA-DR+)	BD Biosciences/G46-6
IFNγ	PE-Cy7	Cytokine-expressing cells	BD Biosciences/B27
Ki67	PerCP-Cy5.5	Proliferating cells	BD Biociences/B56
Ki67	PE	Proliferating cells	BD Biociences/B56

Antibody/Probe	Fluorochromes	Target Population	Vendor/Catalog #/Clone
TNFα	v450	Cytokine-expressing cells	BD Biosciences/MAb11
Anti-vaccinia	Purified	Pathogen-specific cells	Accurate Scientific
Caspase-3	PE	Apoptotic cells	BD Biosciences/C92-605
Fixable Amine Dye	Yellow	Live-dead discriminator, Necrotic cells (Annexin V-/Fixable Amine Viability Dye+)	Invitrogen
Fixable Amine Dye	Aqua		Invitrogen
PARP	FITC	Apoptotic cells	BD Biosciences/F21-852

Isolation of Peripheral Blood Mononuclear Cells

Peripheral blood mononuclear cells (PBMCs) from nonhuman primates were isolated using a Ficoll-Hypaque (GE Health Care Life Sciences, Chicago, IL) procedure. Isolated cells were washed with phosphate buffered saline (Gibco Life Technologies, Thermo Fisher Scientific, Waltham, MA) containing 2% heat-inactivated Hyclone Fetal Bovine Serum (Gibco Life Technologies, Thermo Fisher Scientific, Waltham, MA) and resuspended in media for cell culture to induce apoptosis, cytokine expression, or proliferation.

Flow Cytometer Setup and Optimization of Reagents

Antibody clones used for the development of a multi-color flow cytometry assay are shown in Table 4. Antibodies were titrated, and the stain indices for reagents were calculated to determine optimal titers. The stain index (SI) was calculated by the equation SI = D/W (Maecker and Trotter 2012), where D is the difference of the median values of the positive and negative populations, and W is the spread (2 x rSD) of the negative

population, where rSD is the robust standard deviation value generated in BD FACS Diva software (BD Biosciences, Franklin Lakes, NJ). The greater the value of the SI, the better resolution of the positive and negative cell populations. When possible, the antibody concentration representing the highest SI value were selected, unless this value was greater than the recommended staining volume or cost-prohibitive to scale up to a full-scale nonhuman primate study. The flow cytometer setup, including laser lines and emission filters are shown in Table 5. The flow cytometer had four lasers, including Violet 405nm, Blue 488nm, Green 532nm, and Red 633nm. The laser powers, and emission filters, including long pass and band filters, are shown in Table 5.

Table 5. BD LSR Fortessa flow cytometer configuration

Laser lines	Power (mW)	Fluorochrome	Emission Filters
Violet 405 nm	100	Qdot 705	685LP; 705/70
		Qdot 655	630LP; 660/20
		Qdot 605	595LP; 605/40
		Qdot 585 / Yellow Viability Dye	570LP; 585/42
		Qdot 565	550LP; 560/20
		Qdot 545	535LP; 560/40
		AmCyan / Aqua Viability Dye	505LP; 525/50
		Pacific Blue	450/50
Blue 488 nm	100	PerCP-Cy5.5	670LP; 695/40
		FITC	505LP; 515/20
		SSC	488/10
Green 532 nm	150	PE-Cy7	735LP; 780/60
		PE-Cy5.5	685LP; 710/50
		PE-Cy5	640LP; 670/30
		PE-Texas Red	600LP; 610/20
		PE	575/25
Red 633 nm	100	APC-Cy7	740LP; 780/60
		Alexa700	685LP; 710/50
		APC	660/20

Camptothecin Cultures to Induce Apoptosis

Freshly isolated PBMCs from nonhuman primates were treated with 2 to 10 µLs Camptothecin- (BioVision, Inc., Milpitas, CA) containing media to induce apoptosis (Dolzhanskiy and Bach, 1994). Complete media was prepared using RPMI 1640 (Thermo Fisher Scientific, Waltham, MA) containing sodium pyruvate (Thermo Scientfiic, Waltham, MA) and MEM non-essential amino acids (NEAA) (Thermo Scientfic Waltham, MA), and supplemented with L-glutamine (Thermo Scientific, Waltham, MA), 4-(2-hydroxyethyl)-1-piperazineethanesulfonic acid (HEPES) (Thermo Scientific, Waltham, MA), Gentamicin (Thermo Scientific, Waltham, MA), and 5% heat-inactivated fetal bovine serum (FBS). Cells were cultured at 2E+06 cells/well in a 48-well plate and incubated overnight at 37 degrees Celsius (°C) at 5% carbon dioxide (CO_2). The following day, cells were harvested and washed using 1X AVBB, a calcium-containing buffer, prior to staining for flow cytometry.

Mixed Population Annexin V Transfer Experiments

An experiment was performed mixing populations of cells that were apoptosis-induced, and Annexin V and Aqua ViD stained (Donor), with acceptor cells. Acceptor cells were a population of cells mock-treated (Acceptor (Naïve)). The acceptor population was stained with CD45 and Yellow ViD for discrimination between donor and acceptor mixed-populations. The acceptor cells were pelleted and 1 mL of fluid, either wash buffer or BD Cytofix/Cytoperm, was added. Donor cells (Annexin/Aqua ViD-stained) were added in equal ratio, 275,000 donor cells to 275,000 acceptor cells. Samples were immediately centrifuged and 750 µL of fluid was removed such that the mixed populations were equally concentrated in 250 µL buffer. The samples were vortexed and incubated at

room temperature for 30 minutes. This experimental setup provided a flash-fixation and permeabilization step, with or without calcium added, prior to concentrating the mixed populations. Fixed/permeabilized cells were washed with 1X BD Perm Wash, with or without calcium, prior to flow cytometry. Non-fixed cells were washed prior to flow cytometry with 1X PBS + 2% FBS or 1X AVBB (+Calcium).

Phorbol 12-Myristate 13-Acetate (PMA) /Ionomycin Cultures to Induce Proliferation and Intracellular Cytokine Production

Freshly isolated PBMCs from rhesus monkeys were cultured in complete media supplemented with a low dose of PMA (100 nanograms (ng)/mL; Sigma-Aldrich, St. Louis, MO) and Ionomycin (200 ng/mL; Sigma-Aldrich, St. Louis, MO). The cells were incubated in PMA and Ionomycin for 2 to 4 days at 37°C at 5% CO_2. Cells were harvested and washed using 1X AVBB prior to staining for flow cytometry. Intracellular cytokine expression of TNFα (BD Biosciences, Franklin Lakes, NJ) and interferon gamma (IFNγ) (BD Biosciences, Franklin Lakes, NJ) was induced using freshly isolated PBMCs from nonhuman primates stimulated in Advanced RPMI 1640 media (Thermo Scientific, Waltham, MA) supplemented with PMA and Ionomycin. The cells were incubated in PMA and Ionomycin for 2 hours at 37°C at 5% CO_2 prior to the addition of GolgiPlug (BD Biosciences, Franklin Lakes, NJ) for the remaining 10-12 hour incubation period. Cells were harvested and washed using 1X AVBB prior to staining for flow cytometry.

Detecting Late Apoptosis Using an Amine-Reactive Fixable-Amine Viability Dye

The Amine Reactive Viability Dye Kit (Thermo Scientific, Waltham, MA) was prepared by reconstituting the lyophilized dye in DMSO (kit component). Aliquots were prepared and stored at -20°C. Working stocks were prepared fresh daily, using a 1:20

dilution in 1X PBS, pH 7.4. This reagent was used to measure late apoptosis of rhesus macaque PBMCs at a titered amount that maximized the stain index by flow cytometry.

Bead Preparation for Fluorescence Compensation

Anti-Mouse immunoglobulin G kappa (IgG kappa) beads (BD Biosciences, Franklin Lakes, NJ) and the ArC™ Amine Reactive Compensation Bead Kits (Thermo Scientific, Waltham, MA) were used for compensation. Since Annexin V was not reactive to IgG kappa beads, an IgG1 kappa isotype control was used in a matching fluorochrome from the same vendor for fluorescence compensation.

Staining Cells with Annexin V, Viability Dye, and Monoclonal Antibodies

Cultured cells were harvested into 5-mL round-bottom tubes (BD Falcon, Franklin Lakes, NJ) and washed twice in 1 mL 1X AVBB. Labeling of cells was performed in a 100 µL final volume.

Fixation/Permeabilization Protocol

Cells were gently resuspended prior to the addition of fixation buffers. The following buffers were prepared for testing in combination with Annexin V surface staining: (1) BD Cytofix/Cytoperm (BD Biosciences, Franklin Lakes, NJ), (2) BD Cytofix/Cytoperm supplemented with 1X AVBB (+ Calcium); and (3) BD FACS Permeabilization Solution 2 (BD Biosciences, Franklin Lakes, NJ). Fixation, or fixation and permeabilization, was performed for 30 minutes at room temperature. Non-fixed samples were processed using similar procedural techniques using 1X AVBB (+Calcium). Following fixation, cells were washed twice in 1X BD Perm/Wash solution (BD Biosciences, Franklin Lakes, NJ), supplemented with or without 1X AVBB. The 1X BD

Perm/Wash solution was performed in washing steps to maintain the permeabilized state of the cells.

Intracellular Staining Protocol

Antibody master mixes were prepared in 1X BD Perm/Wash. The total staining volume per reaction was 100 µL. Intracellular staining procedures were performed for 30 minutes to 1 hour at room temperature. Following intracellular staining, cells were washed twice in 1X BD Perm/Wash solution, supplemented with or without 1X AVBB. In some instances, cells were held overnight at room temperature for next day flow acquisition. In other instances, cells were stored at 2-8°C overnight prior to flow cytometry acquisition for up to 2 days. Intracellular isotype controls were vendor-matched to normalize the fluorochrome-to-protein ratio and were also diluted to the same concentration as the test antibody.

Flow Cytometry Acquisition and Analyses

Samples were acquired using a BD LSR Fortessa flow cytometer (Becton Dickinson, Franklin Lakes, NJ) and analyzed using Flow Jo version 10 software (TreeStar Inc. Ashland, OR) or with BD FACSDiva Software (BD Biosciences, Franklin Lakes, NJ).

RESULTS

Two MPXV clades, Congo Basin and West Africa, differ in virulence in nonhuman primates (Saijo *et al.* 2009). Increased virulence of Congo Basin MPXV, relative to West Africa MPXV clade members (Esposito and Fenner 2001, Likos *et al.* 2005), may result from genomic variations that encode VPs that differentially impact host cell responses. Evidence suggests that Congo Basin clade members replicate their viral genomes to higher titers and affect more organ systems than West Africa MPXV clade members (Saijo *et al.* 2009). Furthermore, Congo Basin clade members may inhibit apoptosis, resulting in enhanced viral loads in tissues, as well as necrosis and inflammation. The reduced viral loads in tissues of NHPs exposed to West Africa MPXV (Saijo *et al.* 2009) may be due to efficient apoptosis of pathogen-infected cells. To further explore differences among MPXV clade members in the nonhuman primate model, a flow cytometry assay to study infection and immune regulation, to Zaire 79 (Congo Basin) and Sierra Leone (West Africa) virus strains needed to be developed. Previously, a method of Annexin V/PI or AnnexinV/7-AAD, commonly used for apoptosis detection, did not permit fixation and/or permeabilization for intracellular measurements by flow cytometry. In this thesis, a method for intracellular quantification of immune cells containing MPXV VPs, and immune cells undergoing proliferation, with Annexin V was developed. Furthermore, the Annexin V assay was extended to include intracellular cytokine detection with TNFα and IFNγ.

Annexin V Apoptosis Was Enhanced with Camptothecin + Phorbol 12-Myristate 13-Acetate (PMA) + Ionomycin Cultures

To develop a flow cytometry assay with Annexin V/Fixable-Amine ViD, a method of inducing apoptosis was needed. Treatment with PMA + Ionomycin has commonly been used to stimulate cytokine production, and treatment has also been for immunotoxicity assessments (Ai *et al.* 2013).

Nonhuman primate PBMCs were thawed from frozen, and treated overnight at 37°C with PMA + Ionomycin, or media as a negative control. Phorbol 12-myristate 13-acetate treatment was previously shown to downregulate CD4 expression on the cell surface (Anderson and Coleclough 1993; O'Neil-Anderson and Lawrence 2002; Petersen *et al.* 1992; Ruegg *et al.* 1992), so CD4 was used as a positive-control for PMA + Ionomycin treatment in this experiment. Samples were stained with CD4 and Annexin V to measure apoptosis. Results indicated treatment with PMA + Ionomycin minimally enhanced Annexin V+ apoptosis among lymphocytes (27.2%), relative to media treatment (18.4%) (Figure 8). The CD4+ frequency among lymphocytes was markedly reduced with PMA + Ionomycin treatment (6.97%) relative to the media control (46.4%).

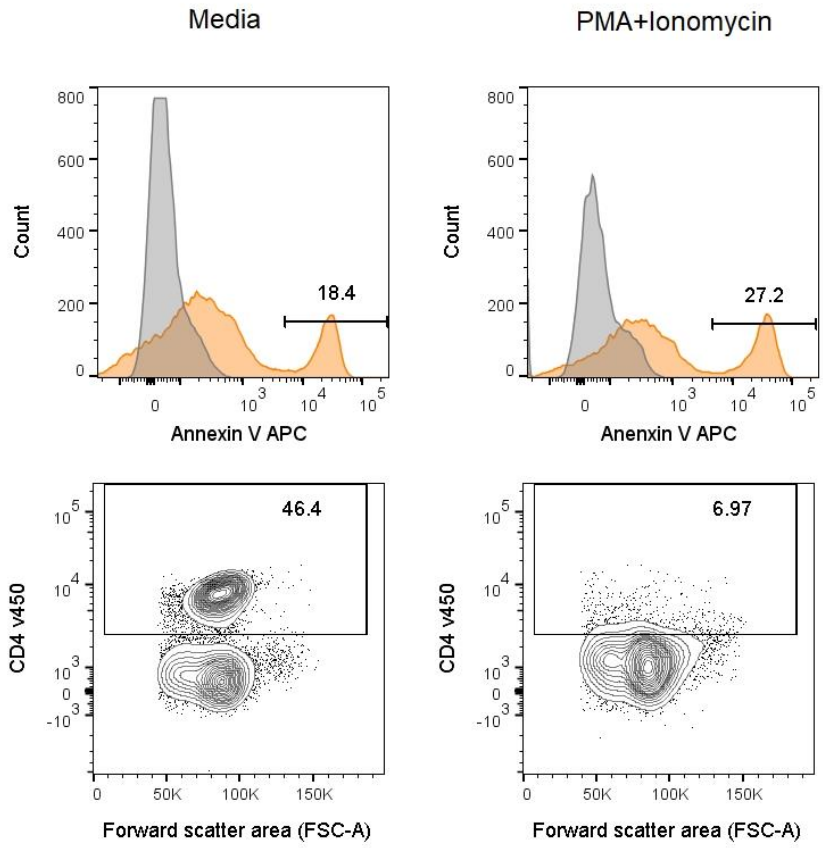

Figure 8. The difference between treatments with PMA + Ionomycin and Media in the induction of apoptosis. Flow cytometry histogram overlays (top row) and contour plots (bottom row) are shown. In the top row, the x-axis shows the logarithmic fluorescent intensity of Annexin V APC, and the y-axis shows the cell count. Histogram gating shows the Annexin V frequencies among gated lymphocytes, for media-treated peripheral blood mononuclear cells (PBMCs) (top left), and for PMA+Ionomhycin-treated PBMCs (top right). Annexin V stained-samples (orange color) are overlayed on top of unstained samples (gray color). In the bottom row, the x-axis shows cell size (Forward scatter area (FSC-A)), and the y-axis shows the logarithmic fluorescent intensity of CD4 v450. The frequencies of CD4 cells among gated lymphocytes are shown. Data was acquired on a BD LSR Fortessa flow cytometer with BD FACS Diva software. Data analysis was performed using Flow Jo v.10.

Camptothecin was previously reported to induce apoptosis of T-lymphoblastoid cells in a dose-dependent manner (Johnson *et al.* 1997). To enhance apoptosis among lymphocytes, Camptothecin, a DNA topisomerase I inhibitor and anti-cancer compound, was tested on NHP PBMCs at 2 micromolar (μM) concentration for an overnight incubation. Nonhuman primate PBMCs were treated with Camptothecin, or PMA + Ionomycin + Camptothecin, or PMA + Ionomycin. Similar to the previous experiment, media treatment was used as a negative control, and CD4 was used as a positive control for PMA + Ionomycin treatments.

Results revealed Annexin V+ apoptosis among lymphocytes was markedly improved with combined PMA + Ionomycin + Camptothecin treatment (41.4%), relative to treatment with only Camptothecin (23.3%), PMA + Ionomycin (29.9%), or media (11.1%) (Figure 9). Similar to the previous experiment, a discernable reduction in the CD4 frequencies among lymphocytes resulted from PBMC treatments with PMA, such as PMA + Ionomycin (11.2%), and PMA + Ionomycin + Camptothecin (13.6%), relative to Camptothecin (58.4%), or media treatment (54.4%) (Figure 9). This experiment indicated that Camptothecin, unlike PMA+Ionomycin, did not alter CD4 expression on the cell surface, making Camptothecin a valuable choice for inducing apoptosis moving forward since maintaining CD4 expression was desirable.

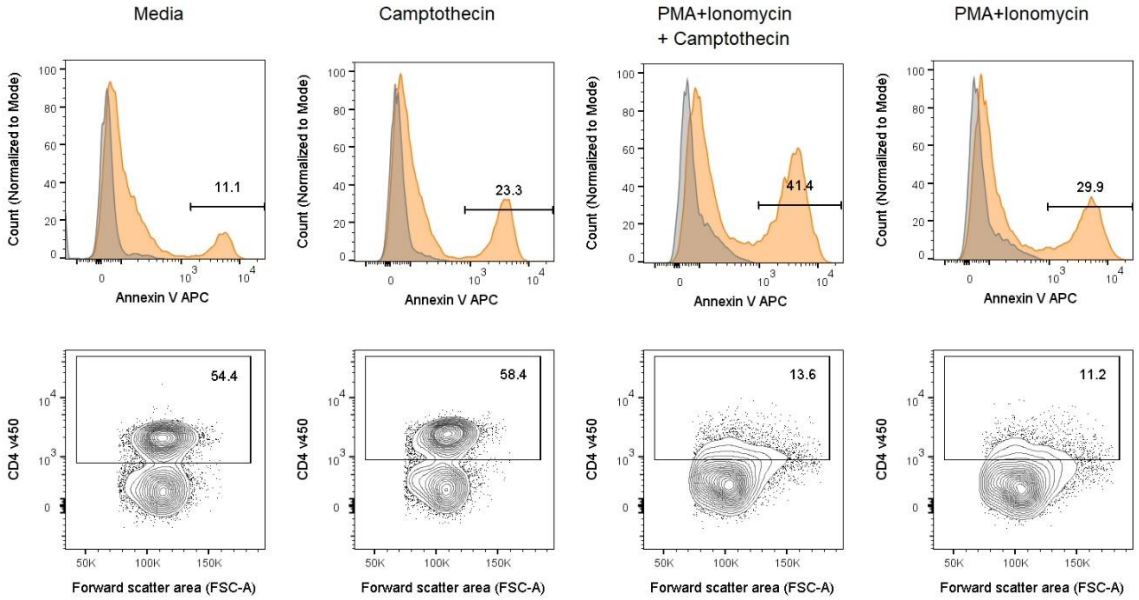

Figure 9. The difference between treatments with Media, Camptothecin, PMA + Ionomycin + Camptothecin, and PMA + Ionomycin in the induction of apoptosis. Flow cytometry histogram overlays (top row) and flow cytometry contour plots (bottom row) are shown. In the top row, the x-axis shows the logarithmic fluorescent intensity of Annexin V APC and the y-axis shows the cell count. Histogram gating shows the Annexin V frequencies among gated lymphocytes for media-treated, camptothecin-treated, PMA+Ionomycin+Camptothecin-treated, and PMA+Ionomycin-treated peripheral blood mononuclear cells (PBMCs). Annexin V-stained samples (orange color) are overlayed on top of unstained samples (gray color). In the bottom row, the x-axis shows cell size (Forward scatter area (FSC-A)) and the y-axis shows the logarithmic fluorescent intensity of CD4 v450. Rectangular gating shows the frequencies of CD4 cells among gated-lymphocytes. Data was acquired on a BD LSR Fortessa flow cytometer with BD FACS Diva software. Analysis was performed using Flow Jo v.10.

Apoptotic Stimuli Differentially Regulated Annexin V+ Apoptosis and Necrosis of Lymphocyte Subsets

Flow cytometry assays were performed to further understand effects of various apoptotic-treatments on lymphocyte subsets. Nonhuman primate PBMCs were cultured overnight with Media, Camptothecin, PMA+Ionomycin, or PMA+Ionomycin+Camptothecin. The effects of treatments were observed among CD4+ T-cells (Lymph\CD3+CD20-\CD4+CD8-), CD8+ T-cells (Lymph\CD3+CD20-\CD8+CD4-), B cells (Lymph\CD3-CD20+), and NK cells (Lymph\CD3-CD16+). Quadrant gating for these experiments were based on a fluorescence-minus-one control for Annexin V, in order to define apoptotic cells (Annexin V+/ViD Yellow-), necrotic cells (Annexin V-/ViD Yellow+), and healthy cells (Annexin V-/ViD Yellow) (Figure 10).

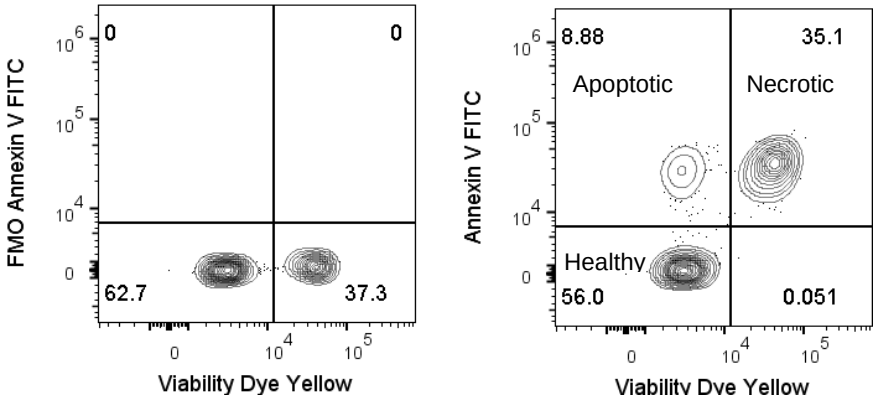

Figure 10. Representative quadrant gating of apoptotic and necrotic cells using Annexin V and Fixable-Amine Viability Dye (ViD). Representative flow cytometry contour plots gated on lymphocytes/CD4+ are shown. Quadrant gating shows apoptotic cells (Annexin V+/ViD Yellow-) in the upper left quadrant, and necrotic cells (Annexin V-/ViD Yellow+) in the upper right quadrant. Healthy cells are shown in the bottom left quadrant. Quadrant gating was based on a Fluorescence-Minus-One (FMO) control for Annexin V FITC. Data was acquired on a BD LSR Fortessa flow cytometer with BD FACS Diva software. Analysis was performed using Flow Jo v.10.

Results showed that Camptothecin-treatment predominantly induced apoptosis and necrosis of CD4+ and CD8+ T-cells. Among CD4+ T-cells, three times more necrosis occurred than apoptosis. Among CD8+ T-cells, levels of necrosis and apoptosis were relatively similar. PMA+Ionomycin+Camptothecin-treatment induced necrosis of CD8+ T-cells, but did little to activate apoptosis. Effects of PMA+Ionomycin+Camptothecin could not be measured on CD4+ T-cells due to downregulation of CD4 expression, or on NK cells due to low cell numbers (< 200 gated CD16+CD3- cells). Apoptosis was greatly increased among B cells with PMA+Ionomycin+Camptothecin, and necrosis was remarkably reduced relative to levels observed in the PBMCs treated with media control or other apoptotic stimuli. Camptothecin treatment alone had little effect on B cells or NK cells (Figure 11).

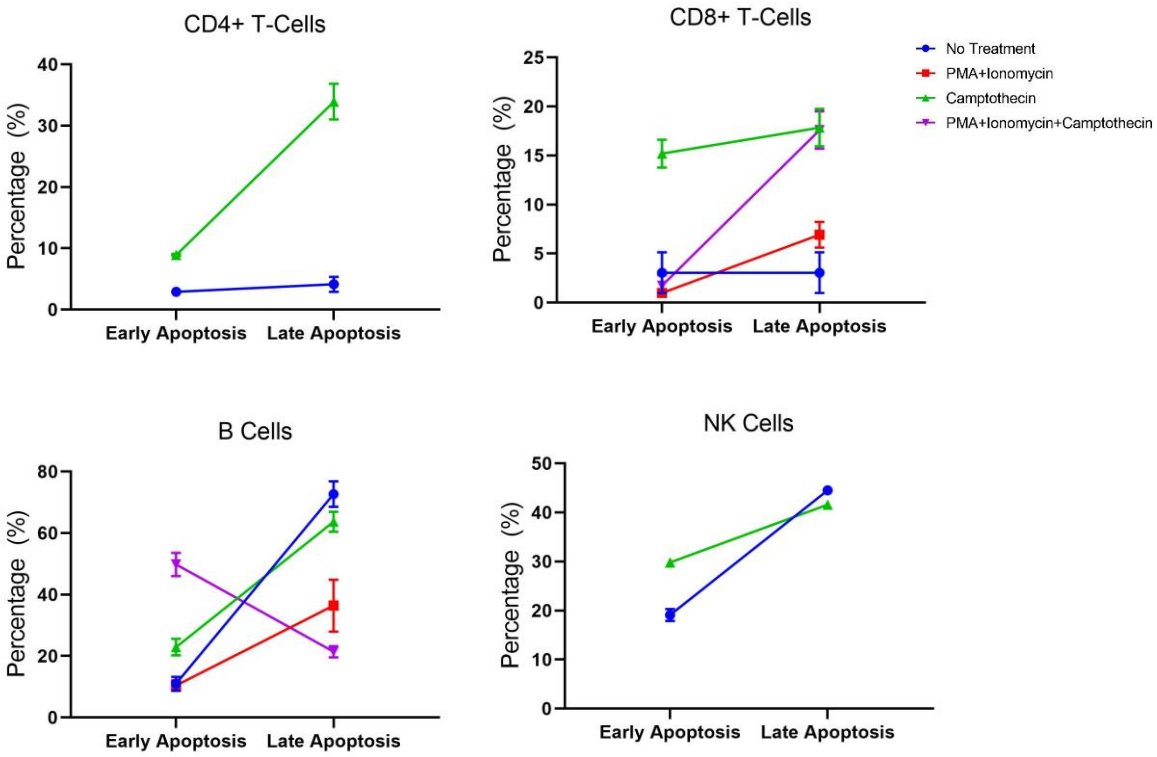

Figure 11. The effect of apoptotic stimuli on CD4+ and CD8+ T-cells, B cells, and NK cells. Graphs with superimposed symbols and connect line are shown for No Treatment (blue circles), PMA+Ionomycin (red squares), Camptothecin (green triangles), and PMA+Ionomycin+Camptothecin (purple triangles). Peripheral blood mononuclear cells were treated overnight and stained for immune cell subset identification. The x-axis is the classification of cells based on staining with Annexin V and Fixable-Amine Viability Dye (ViD): Apoptotic cells (Annexin V+/ViD Yellow-) are shown on the left and Necrotic cells (Annexin V-/ViD Yellow+) are shown on the right of the x-axis. The y-axis is the frequency of apoptotic or necrotic cells among gated-immune cell subsets. Data was acquired on a BD LSR Fortessa flow cytometer with BD FACS Diva software. Analysis was performed using Flow Jo v.10. Graphs were generated in GraphPad Prism 8.

Annexin V Detection Was Compatible with BD Cytofix/Cytoperm reagents

For studies with MPXV, a Biosafety Level 3 (BSL-3) category pathogen, cells must be fixed to inactivate virus prior to data acquisition. Fixation and permeabilization of cell membranes must also be performed for intracellular quantification of cellular proliferation by Ki67, and for MPXV detection within immune cells.

A flow cytometry experiment was performed to study the effect of fixation and permeabilization reagents on Annexin V frequencies among lymphocytes. Nonhuman primate PBMCs were stimulated overnight with Camptothecin, or PMA+Ionomycin+Camptothecin, at 37°C. The following day, PBMCs were harvested and washed twice with 1X AVBB (+Calcium), and then incubated with surface antibodies and proteins. Finally, PBMCs were fixed, or fixed and permeabilized with BD Cytofix, BD Cytofix/Cytoperm, or BD Permeabilization Solution 2 reagents. Non-fixed samples were processed in parallel, using similar techniques, but 1X AVBB (+Calcium) was substituted in place of fixation buffer. Flow cytometry was performed and Annexin V+ frequencies among gated lymphocytes was measured among unfixed PBMCs and PBMCs treated with common fixation and permeabilization reagents (Table 6). Flow cytometry analysis revealed similar Annexin V+ frequencies among gated lymphocytes from NHP PBMCs fixed with BD Cytofix, or fixed and permeabilized with BD Cytofix/Cytoperm, relative to unfixed PBMCs. In contrast, a marked reduction in Annexin V resulted from fixation and permeabilization of PBMCs with BD Permeabilization Solution 2.

Camptothecin-treated NHP PBMCs had similar Annexin V+ frequencies among gated lymphocytes when fixed with BD Cytofix or BD Cytofix/Cytoperm reagents (35.1% No Fixation, 35.3% BD Cytofix, and 35.2% BD Cytofix/Cytoperm). In contrast, the Annexin V+ frequency was 16.8% with BD Permeabilization Solution 2 treatment, roughly one-half of the Annexin V frequency of the unfixed gated-lymphocytes (35.1%) (Table 6). Nonhuman primate PBMCs treated with PMA + Ionomcyin + Camptothecin, had comparable Annexin+ frequencies among lymphocytes, when fixed with BD Cytofix or BD Cytofix/Cytoperm reagents (52.0% No Fixation, 57.5% BD Cytofix, and 56.9% BD

Cytofix/Cytoperm). With BD Permeabilization Solution 2 treatment, the Annexin V+ frequency among lymphocytes was 18.3%, approximately one-third of the Annexin V frequency of the unfixed sample (52.0%) (Table 6). Taken together, these data indicate that Annexin V apoptosis detection was compatible with BD Cytofix/Cytoperm reagents, but not BD Permeabilization Solution 2.

Table 6. The effect of fixation and fixation/permeabilization on Annexin V expression among lymphocytes

Gated Population	Treatment	No Fixation	BD Cytofix	BD Cytofix/ Cytoperm	BD Permeabilization Solution 2
		Annexin V (%)	Annexin V (%)	Annexin V (%)	Annexin V (%)
Lymphocytes	Camptothecin	35.1	35.3	35.2	16.8
	PMA + Ionomycin + Camptothecin	52.0	57.5	56.9	18.3

Calcium Removal Resulted in Annexin V Detachment from Phosphatidylserine

Previously, Tait and Gibson reported that, when calcium was removed from the binding interaction, Annexin V detached from PS on erythrocytes (Tait and Gibson 1994). To visualize the detachment of Annexin V from PS among lymphocytes, NHP PBMCs were stimulated with 2 µM Camptothecin overnight, washed with 1X AVBB (+Calcium), and stained with Annexin V. The sample was equally split into two samples. Prior to flow cytometry acquisition, the first sample was washed with 1X AVBB (+Calcium), and the second was washed with 1X PBS + 2% FBS (-Calcium) (Figure 12). The gating strategy used for live, lymphocytes was SSC-A/FSC-A, followed by ViD Aqua-/SSC-A (Figure

12A). Twenty-five percent of live, lymphocytes bound Annexin V in the presence of calcium; however, Annexin V decreased 15%, to a frequency of 9.92%, when calcium was removed from the binding interaction (Figure 12B). Therefore, these data indicated calcium removal had a pronounced effect on Annexin V detachment from PS among live, lymphocytes (Figure 12).

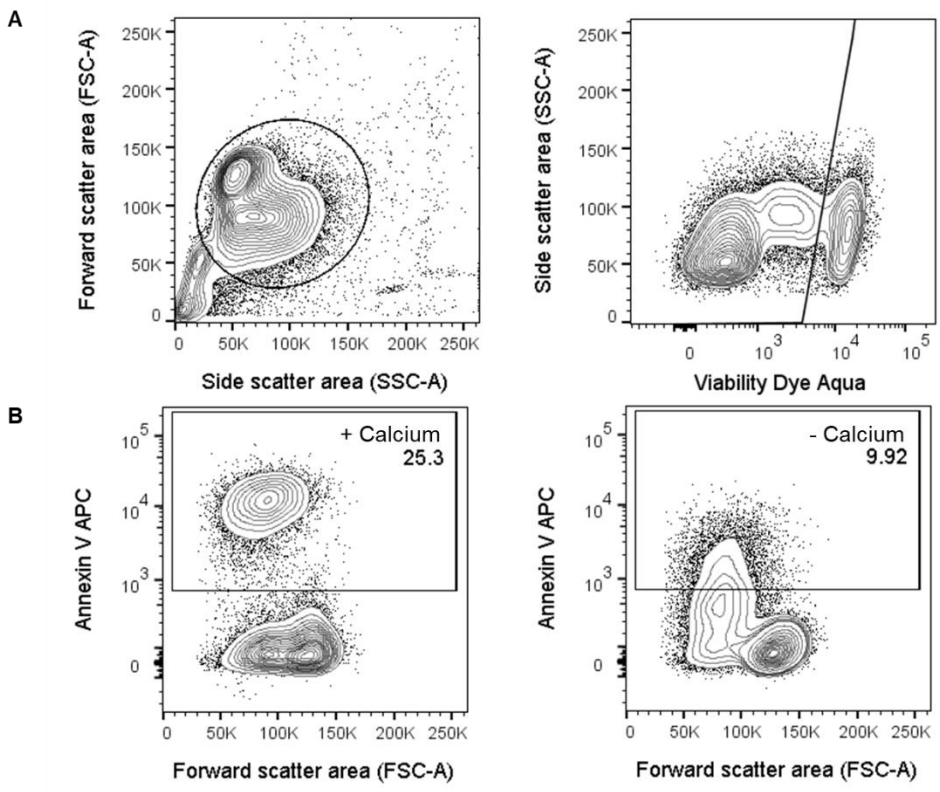

Figure 12. The impact of calcium removal from the Annexin V binding interaction with phosphatidylserine. Flow cytometry contour plots are shown with (A) the gating strategy to analyze live, lymphocytes (SSC-A/Viability Dye Aqua-), excluding dead cells from the analysis, and (B) to examine the frequency of Annexin V+ staining among live lymphocytes when samples were washed in buffers with (+Calcium), and without calcium (-Calcium). Samples were acquired on a BD LSR Fortessa flow cytometer with BD FACS Diva software. Analysis was performed using Flow Jo v.10.

Annexin V+ Frequencies Among Lymphocytes and CD3+ T-Cells Were Similar in Intracellular Assay Steps, Regardless of the Presence of Calcium

Since Annexin V binding to PS was reversible among lymphocytes upon removal of calcium, the effect of calcium in intracellular assay steps for flow cytometry using BD Cytofix/Cytoperm and BD Perm Wash reagents needed to be determined. A flow cytometry assay with Annexin V combined with intracellular staining had not been published, and uncertainty existed among members of the flow cytometry community regarding reliable quantitation of Annexin V apoptosis in combination with intracellular assay procedures.

Therefore, the relationship between omission of calcium in intracellular assay steps for flow cytometry (e.g., fixation and permeabilization and intracellular washing steps) and the stability of Annexin V expression among lymphocytes and CD3+ T-cells was explored (Table 7). Nonhuman primate PBMCs were treated with media, or treated with 5 µM Camptothecin overnight to induce apoptosis. Samples were stained with Annexin V and CD3. Intracellular assay steps, including fixation/permeabilization and intracellular washes were performed without calcium, prior to flow cytometry acquisition.

Here, omission of calcium in the fixation and permeabilization and intracellular assay steps resulted in negligible changes in Annexin V frequencies among lymphocytes, and among CD3+ T cells, at days 0 (same day acquisition) and 1 (next day acquisition). With Camptothecin treatment, the Annexin V frequencies were 61.0% and 59.6% among lymphocytes, and 35.7% and 33.9% among CD3+ T-cells, at days 0 and 1, respectively. Samples treated with media had Annexin V frequencies among lymphocytes of 23.3% and

21.8%, at days 0 and 1, respectively. The media-treated cells had Annexin V frequencies among CD3+ T-cells of 7.11% and 6.41% at days 0 and 1, respectively.

Table 7. Annexin V expression and stability on lymphocytes and CD3+ T-cell populations when calcium was omitted from fixation/permeabilization and intracellular assay procedures. To determine stability of Annexin V, samples were acquired the same day, and then held overnight at room temperature and acquired the next day.

Gated Population	Treatment	Same Day Acquisition Annexin V (%)	Next Day Acquisition Annexin V (%)
Lymphocytes	Media	23.3	21.8
	Camptothecin	61.0	59.6
CD3+ T-cells	Media	7.11	6.41
	Camptothecin	35.7	33.9

Next, Annexin V was tested in combination with intracellular assay steps while calcium was held constant throughout all steps. Nonhuman primate PBMCs, from a different nonhuman primate, were treated with media, or treated with 5 µM Camptothecin to induce apoptosis. Samples were stained with Annexin V and CD3, and fixed and permeabilized with BD Cytofix/Cytoperm containing 1X AVBB (+Calcium). Samples were washed with 1X BD Perm/Wash containing 1X AVBB (+Calcium). Samples were acquired at the flow cytometer, and then acquired the following day, so Annexin V stability could be assessed. The samples were held overnight at room temperature for Annexin V stability measurements. Fixation and permeabilization and intracellular assay steps with

calcium resulted in negligible changes in Annexin V frequencies among lymphocytes, and among CD3+ T cells, at days 0 and 1.

Regardless of the presence or omission of calcium in the intracellular assay steps, negligible changes in frequencies of Annexin V among lymphocytes and CD3+ T cells were observed at day 1 relative to day 0. When calcium was held constant (Table 8), lymphocytes from samples treated with media had Annexin V frequencies of 29.2% and 32.5% at days 0 and 1, respectively. With Camptothecin treatment, the Annexin V frequencies were 62.3% and 64.2% among lymphocytes at days 0 and 1, respectively. Frequencies of Annexin V at days 0 and 1, among CD3+ T-cells from media-treated samples, were 16.4% and 15.2%, respectively. With Camptothecin treatment, Annexin V frequencies at days 0 and 1 among CD3+ T-cells, were 49.4% and 52.6%, respectively.

Table 8. Annexin V expression and stability on lymphocytes and CD3+ T-cell populations when calcium was held constant throughout fixation/permeabilization and intracellular assay procedures

Gated Population	Treatment	Same Day Acquisition Annexin V (%)	Next Day Acquisition Annexin V (%)
Lymphocytes	Media	29.2	32.5
	Camptothecin	62.3	64.2
CD3+ T-cells	Media	16.4	15.2
	Camptothecin	49.4	52.6

Pronounced and Specific Ki67 Proliferation Was Observed With an Overnight Rest Prior to Flow Cytometry Acquisition

Concurrently, with the previous experiment, additional PBMCs were treated with PMA+Ionomcyin for forty-eight hours and stained with Ki67, an intracellular marker for cellular proliferation. During this experiment, the discovery was made that pronounced, and specific, Ki67 staining resulted from holding samples overnight for next-day flow cytometry acquisition (Table 9). Samples were stained with Ki67 PerCP-Cy5.5 or Ki67 PE, and vendor- and concentration-matched isotype controls were used to assess non-specificity, or background. Two fluorochromes were tested for Ki67 staining, PE and PerCP-Cy5.5, and the trend was similar between these reagents, with enhancement of staining observed at day 1 (next day acquisition) relative to day 0 (same day acquisition) (Table 9).

Pronounced, and specific, Ki67 staining was observed at day 1 (next day flow cytometer acquisition) relative to day 0 (same day flow cytometer acquisition). Staining with Ki67 PerCP-Cy5.5 resulted in a greater frequency of proliferating cells relative to Ki67 PE. At day 1, the Ki67 PerCP-Cy5.5-stained sample detected a greater frequency of proliferative lymphocytes (54.1%) than the PE-stained sample (20.3%). Ki67 PE frequencies among lymphocytes were 10 times greater at day 1 (20.3%) relative to day 0 (2.27%), whereas Ki67 PerCP-Cy5.5 frequencies were 5 times greater. However, the PerCP-Cy5.5-stained sample had a greater frequency of proliferative lymphocytes at days 0 (10.0%) and 1 (54.1%), relative to the PE-stained sample at days 0 (2.27%) and 1 (20.3%). Intracellular isotype controls were used to measure non-specific binding and confirm Ki67 staining was specific. IgG1 isotype control frequencies remained relatively

unchanged. The isotype control PerCP-Cy5.5 frequencies among lymphocytes for same day and next day acquisition were both 0.54%. The isotype control PE frequencies among lymphocytes for same day and next day acquisition were 0.29% and 1.50%, respectively. Since Ki67 staining was enhanced following an overnight rest prior to flow cytometry acquisition, the length of the assay was adjusted accordingly.

Table 9. The effect of holding samples overnight at room temperature and next day sample acquisition on Ki67 expression among lymphocytes as measured by Ki67 PE and Ki67 PerCP-Cy5.5 and isotype controls

Gated Population	Antibody	Same Day Acquisition Proliferation (%)	Next Day Acquisition Proliferation (%)
Lymphocytes	Ki67 PerCP-Cy5.5	10.0	54.14
	Ki67 PE	2.27	20.3
	IgG1 PerCP-Cy5.5	0.54	0.54
	IgG1 PE	0.29	1.50

Annexin V Was Stable Upon Fixation/Permeabilization, For Up to Two Days at 2-8°C, Regardless of the Presence of Calcium

Since the length of the assay had to be extended for detection of Ki67, experiments were designed to determine whether Annexin V was stable for up to 2 days at 2-8°C. This would enable the Annexin V assay to be extended past the overnight incubation required for Ki67 detection, and permit holding the sample for an extra day at 2-8°C due to unforeseen circumstances, for flow cytometry acquisition.

Results indicated that two days of storage at 2-8°C had little to no effect on the frequency of Annexin V+ early apoptotic lymphocytes (Annexin V+/Yellow ViD-), regardless of whether samples were unfixed, or fixed and permeabilized in the presence or absence of calcium-supplemented buffer. Without fixation, the frequency of Annexin+ early apoptotic lymphocytes minimally decreased from 5.33% at day 0 to 4.56% at day 2 (difference = -0.77%). With fixation and permeabilization in the presence of calcium-containing buffer, the frequencies of Annexin V early apoptotic lymphocytes was relatively unchanged (difference = 0.06%; Day 0 = 5.82%; Day 2 = 5.88%). When calcium was omitted from the fixation and permeabilization reaction, the frequency of Annexin V early apoptotic lymphocytes was also relatively unchanged at day 2 (difference = -0.30%; Day 0 = 6.32%; Day 2 = 6.02%).

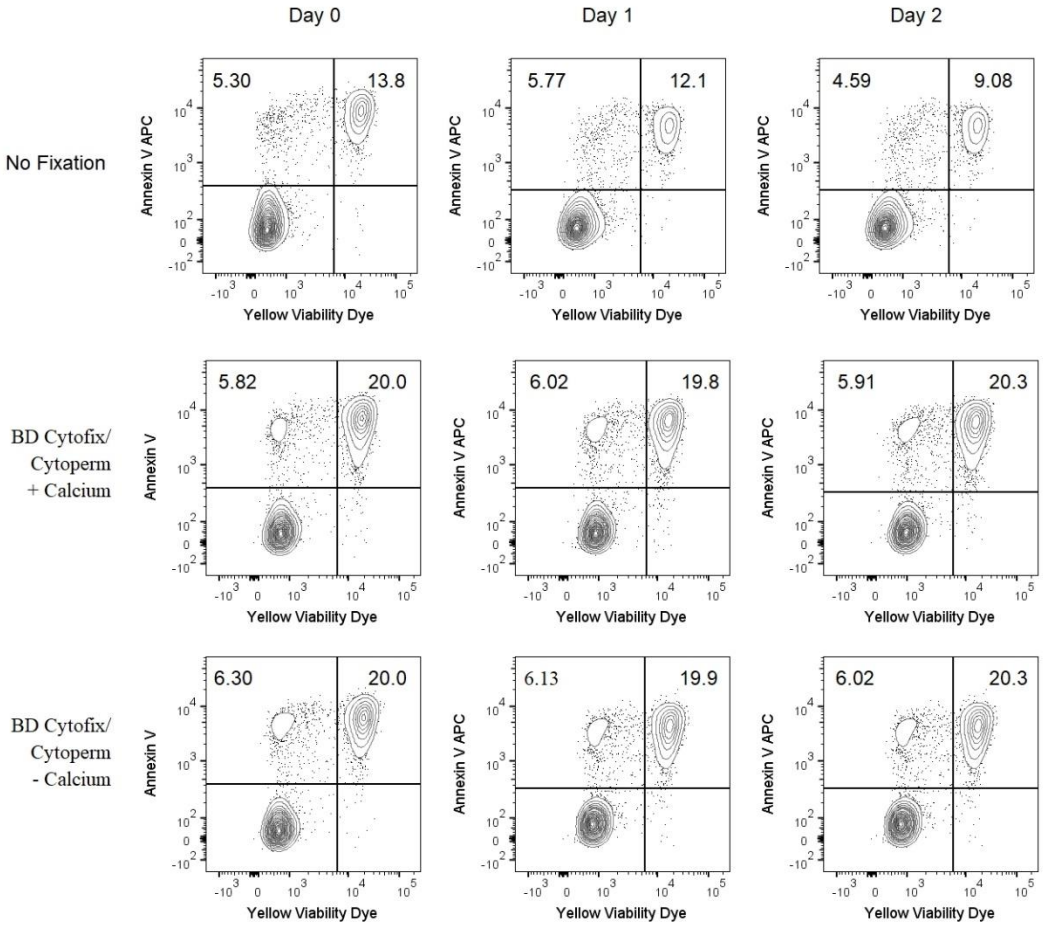

Figure 13. The relationship between treatment with BD Cytofix/Cytoperm, with or without added calcium, and storage time at 2-8°C, on the frequency of early and late apoptosis among lymphocytes. Flow cytometry contour plots are shown with Yellow Viability Dye on the x-axis and Annexin V APC on the y-axis. The number shown on each plot is the Annexin V+ early apoptotic frequency among gated lymphocytes. Treatments include samples that are unfixed (no fixation), or fixed and permeabilized (BD Cytofix/Cytoperm) in the presence of calcium (+Calcium), or the absence of calcium (- Calcium). The samples were acquired the same day at the cytometer (Day 0), and again after 1 day (Day 1), and 2 days of storage at 2-8°C (Day 2).

Annexin V Frequencies among Lymphocytes Are Not Significantly Changed By Intracellular Assay Steps With or Without Calcium

To test the hypothesis that intracellular assay steps with 1X AVBB (+ Calcium) and without 1X AVBB (-Calcium) were associated with statistically insignificant differences in Annexin V frequencies among lymphocytes, a paired t-test was performed. Intracellular assay steps with 1X AVBB (+ Calcium) or without 1X AVBB (-Calcium) were compared across 5 independent experiments. Annexin V apoptosis was stimulated with 2 to 10 µM Camptothecin in overnight cultures at 37°C to generate a distribution of Annexin V frequencies among lymphocytes. Lymphocyte gating was used followed by Annexin V/Viability Dye gating. Boolean gating was performed to calculate total Annexin V frequencies among lymphocytes for comparisons of intracellular assay steps with 1X AVBB (+ Calcium) and without 1X AVBB (-Calcium).

The + Calcium group (n=10) was associated with an Annexin V frequency Mean = 54.4 (SD = 17.2). By comparison, the - Calcium group (n=10) was associated with an Annexin V frequency Mean = 55.1 (SD = 16.8) (Table 10). To determine if the values were from a Gaussian distribution, a D'Agnostino & Pearson omnibus normality test ($p>0.05$) was utilized and the normal QQ plot was visually observed. The + Calcium and the –Calcium groups were approximately normally distributed for the purposes of conducting a paired t-test. The results of the paired t-test (95% confidence interval; two-tailed) showed no statistically significant effect of addition of 1X AVBB (+ Calcium) or omission of 1X AVBB (- Calcium) in intracellular assay steps for flow cytometry ($t = 0.5174$; $p =0.6174$). The data is represented graphically in figure 14.

Table 10. Determination of the significance of intracellular assay steps with or without calcium on Annexin V frequencies among lymphocytes.

Group	*n*	Mean	Range	Standard Deviation	Standard Error Mean
+ Calcium	10	54.4	25.2 - 78.2	17.2	5.4
- Calcium	10	55.1	25.5 - 75.3	16.8	5.3

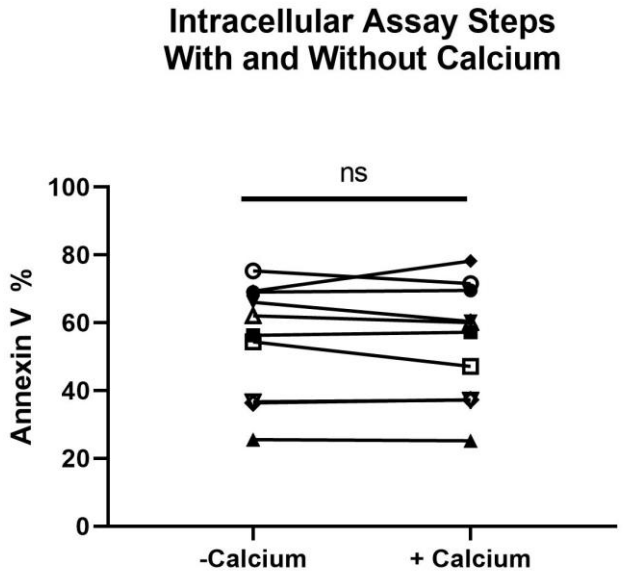

Figure 14. The effect of intracellular assay steps with or without calcium upon Annexin V frequencies among lymphocytes. Graph of superimposed data across 5 independent experiments (n=20) to test the importance of holding calcium (1X Annexin V Binding Buffer) constant throughout all assay steps compared to omitting calcium in intracellular assay steps. The omission (-Calcium) or addition of calcium (+ Calcium) is shown on the x-axis. The frequency of Annexin V among gated lymphocytes is shown (y-axis) for samples treated overnight with 2 to10 micromolar concentrations of Camptothecin overnight at 37°C. Samples were approximately normally distributed based on the D'Agostino & Pearson test for the purposes of conducting a paired t-test (95% confidence interval; two-tailed. The paired t-test (two-tailed; 95% confidence interval) showed no statistically significant difference (ns = non-significant) among calcium addition or omission in intracellular assay steps for flow cytometry (t = 0.5174; p =0.6174).

Intracellular Caspase-3 Staining, With Combined Annexin V Staining, Did Not Permit Caspase-3 Detection When Calcium Was Added To Intracellular Assay Steps

Next, Annexin staining among live, lymphocytes with intracellular Caspase-3 and PARP-1 co-staining was examined. Samples were treated with 10 µM Camptothecin overnight at 37°C, washed with 1X AVBB, and stained with Annexin V, Fixable-amine ViD, CD3, CD8, and CD20. Intracellular assay steps were performed in the presence or absence of calcium, and staining was performed overnight at 2-8°C.

Results showed a noticeable reduction in Caspase-3+/Annexin V+ co-staining from addition of calcium to intracellular assay steps (Figure 15). The Caspase-3+/Annexin V+ frequency was 2.41% when calcium was omitted from intracellular assay steps (BD Cytofix/Cytoperm – Calcium); however, with addition of calcium (BD Cytofix/Cytoperm + Calcium), the frequency was 0.067%. Annexin V+ and Caspase-3 frequencies among lymphocytes were not correlative. Mean Annexin V frequencies among lymphocytes were greater than the Caspase-3 frequency (Annexin V=18.5%; Caspase-3=2.98%). Overall PARP-1 frequencies and Annexin V frequencies were relatively similar (Annexin V=18.5%; PARP-1=15.5%).

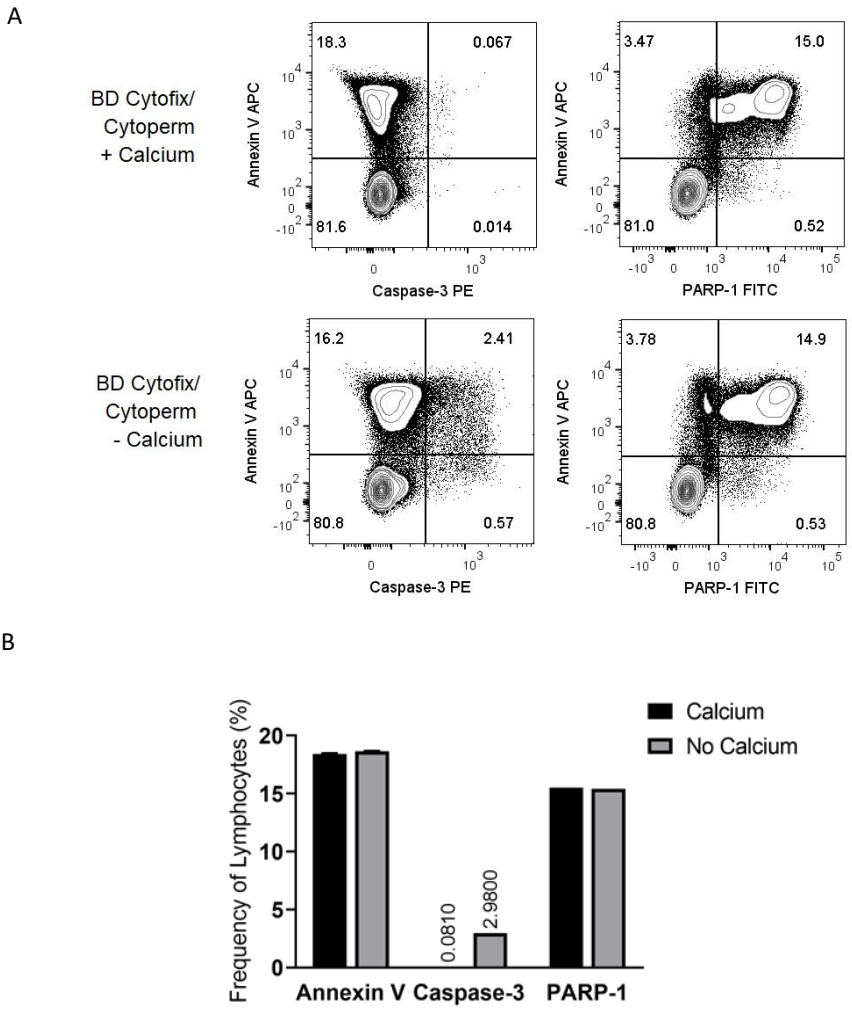

Figure 15. The effect of intracellular washing with BD Perm/Wash, with or without calcium on Caspase-3 and PARP-1 frequencies among live, lymphocytes. (A) Representative contour plots are shown with quadrant gating. Caspase-3 or PARP-1 fluorescent intensities are shown on the x-axis, and Annexin V fluorescent intensities are shown on the y-axis. The quadrant areas are as follows: Upper Left = Caspase-3-/Annexin V+ or PARP-1-/Annexin V+; Upper Right = Caspase-3+/Annexin V+ or PARP-1+/Annexin V+; Lower Right=Caspase-3-/Annexin V- or PARP-1-/Annexin V-; and Lower Right=Caspase-3+/Annexin V- or PARP-1+/Annexin V-. (B) Bar graphs of total frequencies of Annexin V, Caspase-3, and PARP-1, among lymphocytes from (A). Samples were fixed and permeabilized and washed with calcium-containing buffer (+Calcium), or fixed and permeabilized and washed without calcium-containing buffer (-Calcium/No Calcium). Samples were acquired on a BD LSR Fortessa with BD FACS Diva software. Analysis was performed using Flow Jo v.10. Data shown is representative of three independent experiments.

Annexin V Did Not Transfer From a Donor Population to a Naïve-Acceptor Population in a Mixed Population Assay When Calcium Was Removed From Fixation/Permeabilization and Intracellular Assay Steps

In healthy cells not undergoing apoptosis, PS is localized on the inner leaflet of the membrane bilayer, and upon cell permeabilization, Annexin V may dissociate from extracellular PS and associate with intracellular PS resulting in false-positive Annexin V+ events by flow cytometry. Unfortunately, flow cytometry cannot distinguish between Annexin V bound to the inner leaflet of the plasma membrane and the external surface. Since formaldehyde fixation heavily cross-links epitopes, experiments were designed to determine whether fixation/permeabilization maintained Annexin V to PS, regardless of calcium, such that transfer to internal PS would not occur. Mixed population experiments were performed to determine the relationship between fixation/permeabilization with and without calcium, and Annexin V transfer to unoccupied PS sites on the intracellular leaflet of acceptor cells. Donor cells were mixed with acceptor cells in equal ratios. Donor cells were stained with Aqua ViD and Annexin V, such that transfer of Annexin V to an acceptor population could be assessed. Acceptor populations were stained with CD45 PerCP, a pan-hematopoietic marker, and Yellow ViD, to measure transfer of Annexin V to the gated CD45-population. Donor and acceptor cell frequencies in mixed populations were 50 ± 1%, and Annexin V frequencies among the donor cells was approximately 45%. The Annexin V detachment from a donor population and transfer to a naïve, non-Camptothecin-treated acceptor population was assessed (Figure 16). The naïve acceptor population was expected to have few exposed PS sites available on the cell surface; however,

permeabilization would expose intracellular PS sites. The frequency of dead cell staining among the naïve, acceptor population was less than 2% (data not shown).

Results indicated there was no discernible Annexin V transfer from donor populations to naïve acceptor populations among non-fixed or fixed/permeabilized samples. Although Annexin V detached from the non-fixed sample when calcium was removed (-Calcium) (Annexin V+ =10.5%, difference = -32.9%), indiscernible binding to the acceptor population resulted (0.12%) because Annexin V binding to PS requires calcium (Figure 16). Transfer of Annexin V to the intracellular PS sites was not observed.

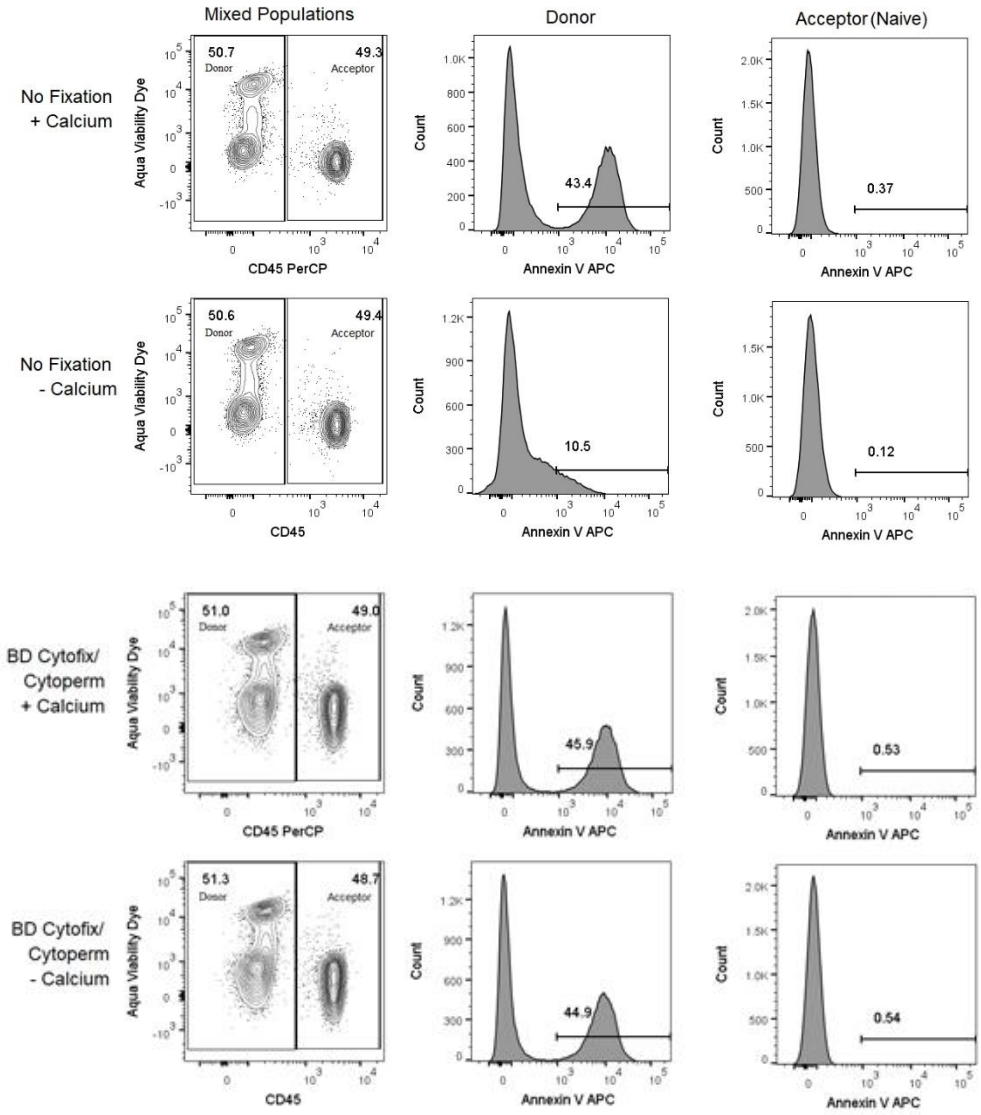

Figure 16. **The relationship between calcium removal and transfer of Annexin V from a donor population to a non-apoptotic, acceptor population.** In mixed population studies, Camptothecin-treated and Annexin V stained donor cells (Donor) were mixed in equal ratios with naïve, untreated acceptor cells (Acceptor (Naïve)). Detachment and transfer of Annexin V was measured for unfixed samples (No Fixation), in the presence of calcium (+Calcium) or omission of calcium (-Calcium) in wash steps. Detachment and transfer of Annexin V was measured for fixed and permeabilized samples (BD Cytofix/Cytoperm), in the presence of calcium (+Calcium) or omission of calcium (-Calcium) in intracellular assay steps. Flow cytometry contour plots (left column) depict the ratio of donor to acceptor cells mixed for each samples' analysis, where the x-axis is CD45, and the y-axis is Aqua Viability Dye. The numbers within the rectangular gates represent the frequency of cells among lymphocytes. Flow cytometry histogram plots (middle column) display Annexin V expression among Donor cells, and Annexin V transferred to acceptor cells (right column). Annexin V is displayed on the x-axis, and count is displayed on the y-axis. Samples were acquired on a BD LSR Fortessa with BD FACS Diva software. Analysis was performed using Flow Jo v.10.

Applications of Intracellular Staining Combined With Annexin V: Proliferation, Cytokines, and MPXV Pathogen Detection

Applications of Annexin V staining among live, lymphocytes, to assess and measure proliferation, intracellular viral MPXV antigens, or cytokines IFNγ and TNFα are shown (Figure 17). Intracellular staining was performed with calcium held constant throughout all assay steps.

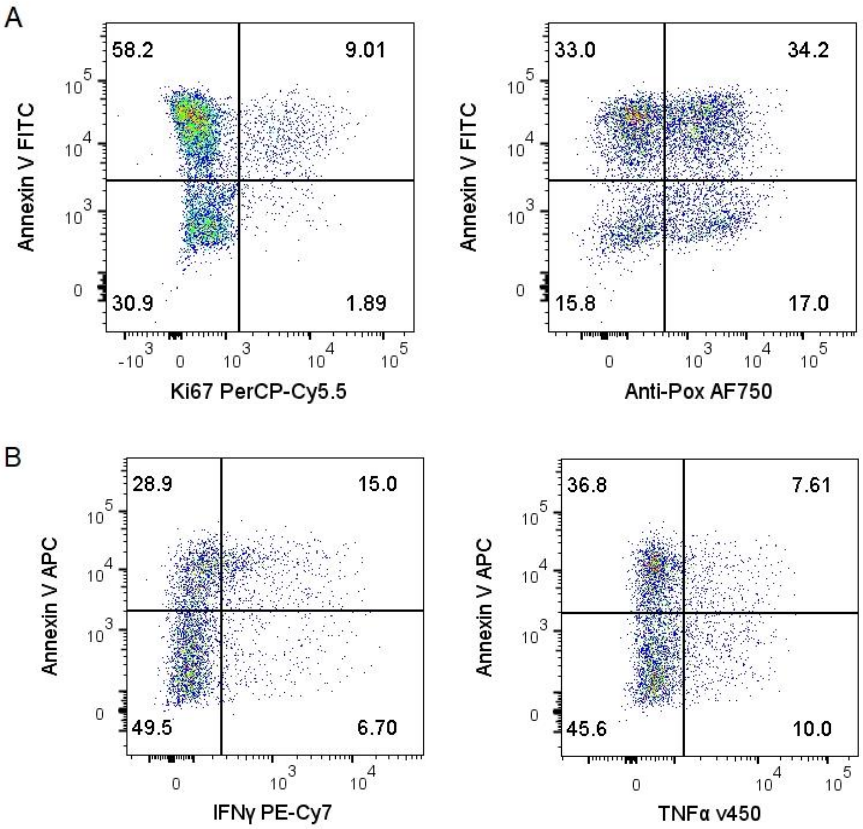

Figure 17. Applications of intracellular staining combined with Annexin V, for analysis of cellular proliferation, viral detection and cytokine analysis by flow cytometry. (A) Bivariate flow cytometry plots are shown with Annexin V on the y-axis and Ki67 or Anti-Pox on the x-axis. Quadrant gating is shown, and the numbers represent the frequencies among gated-lymphocytes. (B) Bivariate flow cytometry plots with Annexin V on the y-axis, and IFNγ or TNFα on the y-axis. Quadrant gating is shown. The numbers on the plots represent the frequencies among gated-lymphocytes. Samples were acquired on a BD LSR Fortessa with BD FACS Diva software. Analysis was performed using Flow Jo v.10.

Immunology Protocols

Contents

1. Description

1. 1 Background Information

This assay was designed to simultaneously examine early and late apoptosis during the course of viral monkeypox infection. Annexin V is a protein that binds to translocated phosphatidylserine during early apoptosis through a calcium-dependent interaction. In this assay, calcium concentration remains constant. Annexin V binding buffer contains calcium and is used in all incubation and wash steps.

Steps **2.1** through **2.3** were designed to be performed at BSL-3. Safety tests were performed with **[Buffer 3]** to enable the assay to be brought to BSL2 for completion and flow cytometry acquisition.

1. 2 Reagent and Instrument requirements

- 700 – 1000 uL EDTA whole blood, per patient
- RPMI 1640 supplemented with 2% FBS at RT
- BD Fortessa Flow Cytometer, Antibodies from **[Supplemental Table 1]** and **[Supplemental Table 2]**.
- ACK Lysis Buffer, Invitrogen

Staining for Apoptosis/Cell Proliferation/Monkeypox-Infected Cells

- **[Buffer 1]:** Yellow Live/Dead Viability Dye (Cat# L34959 / Lot# 802365) *Prepare as follows: 50 uL DMSO, *Room Temp*, added directly to lyophilized Live/Dead Dye *Room Temp*. Prepare 10 uL aliquots and store at –20 ℃. Expiry: 14 Days. Prepare a 1:20 working stock as follows:*

Reagent	Vol. (uL) x # NHPs = Total Vol. (uL)		
Live/Dead Yellow	0.45	20	9.0
PBS, 1X	8.55	20	171.00

Store at 4C, Expiry: 8 hr

- **[Buffer 2]:** Annexin V Binding Buffer, *1X. Dilute to 1X as follows:*

Reagent	Vol. (mL) x #NHPs = Total Vol. (mL)		
Annexin V Binding Buffer, 10X	0.5	20	10.0
diH_20	4.5	20	90.00

Store at 4C, Expiry: 8 hr

- **[Buffer 3]:** BD Cytofix/Cytoperm/ Annexin V Binding Buffer/PFA. *Prepare as follows:*

Reagent	Vol. (mL) x # NHPs = Total Vol. (mL)		
Annexin V Binding Buffer, 10X	0.375	20	7.5
BD Cytofix/ Cytoperm	3.375	20	67.50

Store at 4C, Expiry: 8 hr

Figure 18. Monkeypox study-specific protocol for staining apoptosis, cell proliferation, and pox-infected cells

- **[Buffer 4]:** *(for use at BSL-2)* BD Perm/Wash Buffer/Annexin V Binding Buffer. ***Prepare as follows:***

Reagent	***Vol. (mL) x # NHPs = Total Vol. (mL)***		
Annexin V Binding Buffer, 10X	1	20	20.0
BD Perm/Wash	1	20	20.00
diH_20	8	20	160.0

Store at 4C, Expiry: 8 hr.

2. Protocol for the staining of whole blood for flow cytometry.

2. 1 Lysing the Red Blood Cells (RBCs)

1. Transfer blood to 15 mL conical tubes.
2. Add 4ml ACK buffer. Incubate 2-3 min. at room temp.
3. Bring the volumes to 13ml with PBS. Cfg 250 *x g* for 5 minutes. Aspirate supernatant.
4. wash cells with RPMI containing 2% FBS.
5. Resuspend pellet in 1ml RPMI containing 2% FBS. Incubate at 37°C for **1 hour**.

➢ This incubation is a critical step, and it is so important to rest cells the same amount of time each study day! **Set a timer.**

Upon Entering BSL3:

- Thaw one vial of CPX-V positive control cells (-80°C) in BSL3 37°C water bath until tiny ice chip remains.
- Pour cells into labeled 15mL conical tube and slowly add 5 mL RPMI containing 2% FBS.
- Cfg 850 RPM for 5 minutes. Remove supernatant.
- Resuspend in 1mL RPMI containing 2% FBS.

2. 2 Surface Staining the Blood.

1. Add 3 mL **[Buffer 2]** to each sample tube.
2. Cfg 250 *xg* for 5 minutes. Aspirate supernatant.
3. Resuspend the cells in 150 uL **[Buffer 2]**. Aliquot 50 uL cells into three wells in a U-bottom 96-well plate using **[Supplemental Plate Map 1]**.
4. Aliquot 50 uL of the antibody master mix **[Supplemental Table 1]** into corresponding rows of the plate. To the Unstained Sample, add 50 uL **[Buffer 2]**. Add **3 uL AmCyan**, **2 uL HLA-DR v500**, and **1 uL Annexin V FITC** into individual compensation wells. Gently tap the plate to mix. Incubate plate for 20 minutes at room temp in the dark.
5. Add 100 uL **[Buffer 2]** into each well. Cfg 250 *xg* for 5 minutes. Aspirate supernatant *gently with a multichannel pipet (Please don't spray on plate with microchem).*
6. Resuspend the pellets in 200ul **[Buffer 2].** Cfg 250 *xg* for 5 minutes. Aspirate supernatant *gently with a multichannel pipet.*

2.3 Cell Fixation/Permeabilization

1. Add 150ul **[Buffer 3]** per well. Incubate for at room temp in the dark. Meanwhile, set up a rack of 2mL Sarstedt screw-cap tubes in the same format as the plate. Add 250 uL **[Buffer 3]** per tube.
2. Transfer the samples from the plate to the tubes. Cap the tubes tightly. Spray the rack with 10% microchem. Spray a piece of foil, and wrap the foil around the rack of tubes. Invert tubes to coat entire interior of tube with **[Buffer 3]. Make sure the cells are in Buffer 3 for 30min before taking out to BSL-2 lab.**

➢ ***At this point, the samples can be safely brought to BSL2 to complete the intracellular-staining process.***

2.4 Intracellular Staining at BSL2

1. **Cfg. 500*xg* for 1 min** *to bring all 400 uL of sample to the bottom of the tube. Resuspend cells gently with a pipet before transferring them to the plate in the next step!*
2. Using **[Supplemental Plate Map 2 and 3]**, aliquot 200 uL cells into corresponding wells of the two 96-well U-bottom plates.
3. **Cfg. 500*xg* for 5 mins**. Remove supernatant by quickly flipping the plates into a pan and banking one time on a paper towel.
4. Resuspend cells into 200 uL **[Buffer 4]**.
5. Repeat step 3.
6. Aliquot 50 uL of the antibody master mix **[Supplemental Table 2 and 3]** into corresponding rows of the plate. Tap the plate slightly to mix the wells. Incubate for overnight at 4oC in the dark.

At this point, the samples should be stored in the 4°C refrigerator overnight until the following morning. Please prepare the compensation beads below and also store them in the 4°C refrigerator overnight.

---

7. The next morning, add 150 uL **[Buffer 4]** into each well.
8. Repeat step 3.
9. Add 200 uL **[Buffer 4]** into each well.
10. Repeat step 3.
11. Add anti-rabbit-Alexa750 (1:200) **(Invitrogen A21039, Lot 790312)** 50 uL/well in **[Buffer 4]**. Incubate at RT for I hour in the dark.
12. Add 100 uL **[Buffer 4]** into each well.
13. Repeat step 3.
14. Add 200 uL **[Buffer 4]** to each well of the plate

2.5 Preparing the Samples for Flow Cytometry.

1. Transfer samples to 5 mL flow tubes. Add about 100-200ul more **[Buffer 4]** to each FACS tube to make the volume to about 300-400ul.
2. Acquire the flow the same day.

2.6 Preparing the Compensation Beads

1. Use **[Supplemental Table 4]** to prepare the compensation controls in 5 mL flow tubes.
2. Gently vortex ArC™ Amine Reactive Compensation Bead Kit and BD Compensation Bead Kit components for 30 seconds to completely resuspend before use.
3. Incubate beads with antibody for 15 minutes at room temp in the dark. ArC Negative Beads should NOT be added to the Qdot585 Comp Control.
4. Remember to wash the Qdot 585 Comp Control by adding 3 mL PBS and spinning at 300 *xg*.
5. Finally, add the ArC Negative Beads (Component B) to the tube. And, add 0.5 mL of 1X PBS to each tube.

Supplemental Table 1. *Use the charts below to prepare antibody master mix (right click on table, worksheet object, edit):*

TNK Apoptosis Panel #1

Antibody	*Fluorochrome*	*Volume (µL) x # Tubes* = Total Volume*			*Catalog#*	*Lot#*
CD3	Pacific Blue	2	20	40.0	558124	62605
CD8	APC	3	20	60.0	340659	49901
Annexin V	FITC	1	20	20.0	556419	68690
CD16	PE	5	20	100.0	556619	25566
Live/Dead Dye 1:20	Yellow Qdot 585	2.5	20	50.0	L34959	802365
Buffer, 10X	Annexin V Buffer	5	20	100.0	556454	23025
Buffer, 1X	PBS	31.5	20	630.0	10010072	NA

MNB Apoptosis Panel #2

Antibody	*Fluorochrome*	*Vol. (µL) x # Tubes* = Total Vol. (µL)*			*Catalog#*	*Lot#*
CD14	Pacific Blue	2	20	40.0	558121	63367
Annexin V	FITC	1	20	20.0	556419	68690
CD20	APC	1	20	20.0	641396	69682
CD4	PE	5	20	100.0	550630	73693
Live/Dead Dye 1:20	Yellow Qdot 585	2.5	20	50.0	L34959	802365
Buffer, 10X	Annexin V Buffer	5	20	100.0	556454	23025
Buffer, 1X	PBS	33.5	20	670.0	10010072	NA

DC Apoptosis Panel #3

Antibody	*Fluorochrome*	*Vol. (µL) x # Tubes* = Total Vol. (µL)*			*Catalog#*	*Lot#*
HLA-DR	v500	2	22	44.0	561224	83798
CD3	PACIFIC BLUE	2	22	44.0	558124	62605
CD14	PACIFIC BLUE	2	22	44.0	558121	63367
CD20	eFluor 450	2	22	44.0	48-0209-42	E10608-1630
Annexin V	FITC	1	22	22.0	556419	68690
CD123	PE	2	22	44.0	554529	52757
CD11c	APC	5	22	110.0	340544	75196
Live/Dead Dye 1:20	Yellow Qdot 585	2.5	22	55.0	L34959	802365
Buffer, 10X	Annexin V Buffer	5	22	110.0	556454	23025
Buffer, 1X	PBS	26.5	22	583.0	10010072	NA

Supplemental Table 2. *Use the charts below to prepare antibody master mix (right click on table, worksheet object, edit) :*

1st Ab mix for ICCS staining

Antibody	*Fluorochrome*	*Vol. (µL) x # Tubes* = Total Vol. (µL)*			*Catalog#*	*Lot#*
Ki67	PerCP-Cy5.5	2.5	65	162.5	561284	85033
Anti-Pox	PURIFIED	0.1	65	6.50	YVS8101	H9707
Fc Block	NA	5	65	325.0	120-000-442	5100614305
Buffer 4	NA	42.5	65	2762.5	NA	NA

- Stock concentration of Anti-Pox (Accurate Scientific YVS8101) was diluted to 3mg/mL by Haifeng. The stock concentration of Ki67 PerCP-Cy5.5 is 50 ug/mL.

Isotype control for ICCS 1st Ab mix

Antibody	*Fluorochrome*	*Vol. (µL) x # Tubes* = Total Vol. (µL)*			*Catalog#*	*Lot#*
IgG1 k	PerCP-Cy5.5	0.625	65	40.6	550795	75044
Rabbit IgG	PURIFIED	0.1	65	6.50	AIF403-2	J0632
Fc Block	NA	5	65	325.0	120-000-442	5100614305
Buffer 4	NA	44.3	65	2879.5	NA	NA

- Stock concentration of Rabbit IgG (Accurate Scientific AIF403-2) is 3mg/mL. The stock concentration of IgG_1k PerCP-Cy5.5 is 0.2 mg/mL

Supplemental Table 3. *Use the charts below to prepare antibody master mix (right click on table, worksheet object, edit :*

Compensation Controls Using BD Comp Beads

Sample	*Antibody*	*Vol. (uL) x # Drop Beads**	
UNSTAIN	PBS	2	2
FITC	IgG1	2	2
PE	IgG1	2	2
IgG1 PERCP-Cy5.5	IgG1	2	2
Ki67 PERCP-Cy5.5	Ki67	2	2
APC	CD8	2	2
ALEXAFLUOR 750	CD19	2	2
PACIFIC BLUE	CD14	2	2

* One drop Positive/ One drop Negative

Compensation Controls Using Invitrogen ArC Beads

Sample	*Antibody*	*Vol. (uL) x # Drop Beads**	
QDOT 585	Live Dead Yellow Stock	3	1

* One drop Component A

Compensation Controls Using Cells

Sample	*Antibody*	*Vol. (uL) x Vol. (uL)cells*	
v500*	HLA-DR	2	50
ANNEXIN V**	FITC	1	50

*Cells should be from Uninfected Control

**Cells should be from CPX Pos Control

Supplemental Plate Map 1.

	TNK PANEL			MNB PANEL			DC PANEL					COMP
	1	2	3	4	5	6	7	8	9	10	11	12
A	NHP 1	NHP 9	NHP 17	NHP 1	NHP 9	NHP 17	NHP 1	NHP 9	NHP 17			Annexin Comp
B	NHP 2	NHP 10	NHP 18	NHP 2	NHP 10	NHP 18	NHP 2	NHP 10	NHP 18			Unstain
C	NHP 3	NHP 11	CPX-V POS	NHP 3	NHP 11	CPX-V POS	NHP 3	NHP 11	CPX-V POS			
D	NHP 4	NHP 12		NHP 4	NHP 12		NHP 4	NHP 12	FRESH PBMC			
E	NHP 5	NHP 13		NHP 5	NHP 13		NHP 5	NHP 13	FRESH PBMC			
F	NHP 6	NHP 14		NHP 6	NHP 14		NHP 6	NHP 14				
G	NHP 7	NHP 15		NHP 7	NHP 15		NHP 7	NHP 15				
H	NHP 8	NHP 16		NHP 8	NHP 16		NHP 8	NHP 16				

Supplemental Plate Maps 2 and 3.

Experimental Plate

1ST ANTIBODY MIX FOR ICCS STAINING PANEL

	1	2	3	4	5	6	7	8	9	10	11	12
A	NHP 1	NHP 9	NHP 17	NHP 1	NHP 9	NHP 17	NHP 1	NHP 9	NHP 17			
B	NHP 2	NHP 10	NHP 18	NHP 2	NHP 10	NHP 18	NHP 2	NHP 10	NHP 18			
C	NHP 3	NHP 11	CPX-V POS	NHP 3	NHP 11	CPX-V POS	NHP 3	NHP 11	CPX-V POS			
D	NHP 4	NHP 12		NHP 4	NHP 12		NHP 4	NHP 12	FRESH PBMC			
E	NHP 5	NHP 13		NHP 5	NHP 13		NHP 5	NHP 13	FRESH PBMC			
F	NHP 6	NHP 14		NHP 6	NHP 14		NHP 6	NHP 14				
G	NHP 7	NHP 15		NHP 7	NHP 15		NHP 7	NHP 15				
H	NHP 8	NHP 16		NHP 8	NHP 16		NHP 8	NHP 16				

Isotype Control Plate

ISOTYPE CONTROLS FOR ICCS STAINING PANEL | COMP

	1	2	3	4	5	6	7	8	9	10	11	12
A	NHP 1	NHP 9	NHP 17	NHP 1	NHP 9	NHP 17	NHP 1	NHP 2	NHP 17			Annexin Comp
B	NHP 2	NHP 10	NHP 18	NHP 2	NHP 10	NHP 18	NHP 2	NHP 3	NHP 18			Unstain
C	NHP 3	NHP 11	CPX-V POS	NHP 3	NHP 11	CPX-V POS	NHP 3	NHP 4	CPX-V POS			
D	NHP 4	NHP 12		NHP 4	NHP 12		NHP 4	NHP 5	FRESH PBMC			
E	NHP 5	NHP 13		NHP 5	NHP 13		NHP 5	NHP 6	FRESH PBMC			
F	NHP 6	NHP 14		NHP 6	NHP 14		NHP 6	NHP 7				
G	NHP 7	NHP 15		NHP 7	NHP 15		NHP 7	NHP 8				
H	NHP 8	NHP 16		NHP 8	NHP 16		NHP 8	NHP 9				

Animal_ID	Notes:
NHP 1	
NHP 2	
NHP 3	
NHP 4	
NHP 5	
NHP 6	
NHP 7	
NHP 8	
NHP 9	
NHP 10	
NHP 11	
NHP 12	
NHP 13	
NHP 14	
NHP 15	
NHP 16	
NHP 17	
NHP 18	

DISCUSSION

Two clades of MPXV, Congo Basin and West African, differ in symptom severity and lethality among humans (Esposito and Fenner 2001, Likos et al. 2005). In nonhuman primates, increased virulence was observed with MPXV Congo Basin compared to MPXV West African (Chen et al. 2005). Apoptosis, necrosis, and pyroptosis were previously implicated in *Orthopoxvirus* immunopathogenesis (Wahl-Jensen et al. 2011), but immunopathogenesis among the two MPXV clades had not been studied. To study infection and differential immune response regulation to MPXV Congo Basin (Zaire 79 strain) and MPXV West African (Sierra Leone strain), an assay was developed. In this thesis, an intracellular assay combined with analysis of apoptosis and necrosis with Annexin V/fixable-amine ViD was developed. Previously, the Annexin V/PI method did not permit fixation and/or permeabilization for intracellular measurements (Wlodkowic et al. 2011; ThermoFisher 2019). Here, these data show fixation/permeabilization with BD Cytofix/Cytoperm was compatible with Annexin V. Furthermore, Annexin V was stable upon fixation/permeabilization for up to three days at 2-8°C, the longest time point observed. Annexin detached from PS when calcium was removed, when cells were not fixed. Following fixation/permeabilization, Annexin V frequencies were similar regardless of the presence or absence of calcium in intracellular assay steps. To determine whether Annexin V may detach and transfer to unoccupied PS sites, such as internal PS located inside healthy cells, mixed population studies were performed. When calcium was held constant in fixation/permeabilization, Annexin V detachment and transfer to permeabilized acceptor cells was not observed. Intracellular steps with calcium interfered with antibody detection of cleaved Caspase-3. It is likely the elevated calcium levels used

in intracellular assay steps caused Caspase-3 to undergo a conformational change, which promoted binding of another cytosolic protein (Bobay et al. 2012), thereby blocking antibody detection by anti-Caspase 3. For this reason, investigators should consider studying effects of elevated calcium on intracellular targets of interest prior to designing combined surface and intracellular assays for flow cytometry while holding calcium constant, with Annexin V. In summary, a method was developed for flow cytometry for combined intracellular assay staining, and Annexin V/Fixable-Amine ViD. The development of this assay permitted study of infection and differential immune response regulation to Zaire 79 and Sierra Leone MPXV strains in nonhuman primates.

In the future, this assay may be used to identify to correlates of immunity. Defining strong correlates of immunity would benefit the scientific research community, because efficacy testing of candidate therapeutics and vaccines could be performed with reduced numbers of nonhuman primates. Furthermore, this assay could be modified to study immunopathogenesis of additional infectious BSL-3 or BSL-4 pathogens. Modifications to the assay can easily be made through addition of different antibodies for specific pathogen-detection, or additional cytokines of interest. Here, Annexin V staining is shown in combination with IFNγ and TNFα. The study of cytokines is useful to the study of immune cell function in disease progression, and incorporation of important cytokines into this assay may lead to discovery of immune correlates. Furthermore, pathogen-detection to detect monkeypox VPs inside immune cells was performed using an indirect-staining method. A benefit of indirect staining over direct staining is enhanced signal over background due to increased numbers of secondary antibodies that bind the primary antibody, yielding a greater fluorescence signal. Moving forward, this indirect method

would benefit scientific researchers by enhancing sensitivity of pathogen-detection in the assay. A limitation of the combined Annexin V/Fixable-amine ViD assay; however, is that PS has been expressed on viable monocytes, macrophages, and DCs (Dillon et al. 2001). PS is also highly expressed on activated IL-10 producing B cells (B10 cells), known as B regs (Birge et al. 2016). Binding of Annexin V to extracellular PS on these cells could confound measurements of early apoptosis with Annexin V. This limitation should be considered in the scientific design process when modifying this assay for use.

This work could further be expanded upon by electron microscopy techniques to visualize the transfer of Annexin V to the inner leaflet of the membrane by electron microscopy, if an immunogold-labeled Annexin V protein was available. Additionally, the assay could be expanded upon to measure more fluorescence parameters to capture more information within one sample. The capture of more information is preferred, because sample volumes are often limited in nonhuman primate studies. Pathogens, such as MPXV, may exploit regulatory cells, such as T-regs, to regulate immunosuppression of effector CTLs, thereby enhancing virulence. Perhaps, in Zaire 79 and Sierra Leone MPXV, differential responses of T-regs in MPXV will be studied to elucidate differential regulatory cell functions.

In summary, the assay developed in this thesis may benefit the scientific research community in understanding immunomodulatory properties of MPXV clade members and differential host cell responses. A better understanding in these areas is expected to aid in the design of more, specific-vaccines and targeted therapeutics. Moving forward, it is also possible that the method described in this thesis will be used to discover immune correlates

of protection, reducing the numbers of nonhuman primates needed for *in vivo* efficacy studies.

REFERENCES

Acs B, Kulka J, Kovacs KA, Teleki I, Tokes AM, Meczker A, Gyorffy B, Madaras L, Krenacs T, Szasz AM. 2017. Comparison of 5 Ki-67 antibodies regarding reproducibility and capacity to predict prognosis in breast cancer: does the antibody matter? Hum Pathol. 65: 31-40.

Ai W, Li H, Song N, Li L, Chen H. 2013. Optimal method to stimulate cytokine production and its use in immunotoxicity assessment. Int J Environ Res Public Health 10(9):3834-3842.

Aragon TJ, Ulrich S, Fernyak S, Rutherford GW. 2003. Risk of serious complications and death from smallpox vaccination: A systematic review of the United States experiences, 1963-1968. BMC Public Health 3(26) Published 2003 Aug 11. doi:10.1186/1471-2458-3-26

Anderson SJ, Coleclough C. 1993. Regulation of CD4 and CD8 expression on mouse T cells. Active removal from the cell surface by two mechanisms. J Immunol. 151(10):5123-5134.

Arita I, Jezek Z, Khodakevich L, Ruti K. 1985. Human monkeypox: a newly emerged orthopoxvirus zoonosis in the tropical rain forests of Africa. Am J Trop Med Hyg 34(4):781-789.

Banchereau J, Bazan F, Blanchard D, Briere F, Galizzi JP, van Kooten C, Liu YJ, Rousst F, Saeland S. 1994. The CD40 antigen and its ligand. Annu. Rev Immunol 12:881–922.

BarlogieB, Latreille J, Freireich EJ, Fu CT, Mellard D, Meistrich M, Andreeff M. Characterization of hematologic malignancies by flow cytometry. Blood Cells 6(4):719-44.

Belongia EA, Naleway AL. 2003. Smallpox vaccine: The good, the bad, and the ugly. Clin Med Res 1(2):87-92.

Birge RB, Boeltz S, Kumar S, Carlson J, Wanderley J, Calianese D, Barcinski M, Brekken RA, Huang X, Hutchins JT, Freimark B, Empig C, Mercer J, Schroit AJ, Schett G, Herrmann M. 2016. Phosphatidylserine is a global immunosuppressive signal in efferocytosis, infectious disease, and cancer. Cell Death & Differentiation 23:962–978.

Blasco R, Moss B. 1991. Extracellular vaccinia virus formation and cell-to-cell virus transmission are prevented by deletion of the gene encoding the 37,000-Dalton outer envelope protein. J Virol 65(11):5910-20.

Bobay BG, Stewart AL, Tucker AT, Thompson RJ, Varney KM, Cavanagh J. 2012. Structural insights into the calcium-dependent interaction between calbinding-D28K and caspae-3. FEBS Letters 586:3582–3589.

Bray M. 2003. Pathogenesis and potential antiviral therapy of complications of smallpox vaccination. Antivir Res 58:101-114.

Breman JG, Kalisa-Ruti, Steniowski MV, Zanotto E, Gromyko AI, Arita I. 1980. Human monkeypox, 1970-79. Bull Wld Hlth Org 58(2):165-182.

Cann, AJ. 2012. Principles of Molecular Virology [Internet]. Waltham (MA): Academic Press; [cited 2018 Dec 26]. Available from: https://www.researchgate.net/profile/Akila_Wijerathna_Yapa2/post/Which_is_the_best_book_to_study_molecular_virology/attachment/59d6207c79197b807797ef1d/AS%3A273680301527040%401442261876240/download/Alan_J._Cann_Principles_of_Molecular_Virology.PDF

Centers for Disease Control and Prevention (CDC). 2003. Update: multistate outbreak of monkeypox--Illinois, Indiana, Kansas, Missouri, Ohio, and Wisconsin, 2003. MMWR Morb Mortal Wkly Rep 52(27):642-646.

Centers for Disease Control and Prevention (CDC). [Internet]. [updated 2019 Jan 22]. Smallpox prevention and treatment; [cited 2019 Apr 07]. Available from: https://www.cdc.gov/smallpox/prevention-treatment/index.html

Chen N, Li G, Liszewski MK, Atkinson JP, Jahrling PB, Feng Z, Schriewer J, Buck C, Wang C, Lefkowitz EJ, Esposito JJ, Harms T, Damon IK, Roper RL, Upton C, Buller RML. 2005. Virulence differences between monkeypox virus isolates from West Africa and Congo basin. Virology 340:46-63.

Colamonici OR, Domanski P, Sweitzer SM, Larner A, Buller RM. 1995. Vaccinia virus B18R gene encodes a type I interferon-binding protein that blocks interferon alpha transmembrane signaling. J Biol Chem 270(27):15974-8.

Cono J, Case CG, Bell DM, Centers for Disease Control and Prevention (CDC). 2003. Smallpox vaccination and adverse reactions. Guidance for clinicians. MMWR Recomm Rep 52(RR-4):1-28.

Dillon SR, Constantinescu A, Schlissel MS. 2001. Annexin V binds to positively selected B cells. J Immunol 166(1):58-71.

Dolzhanskiy A, Bach RS. 1994. Flow cytometric determination of apoptosis in heterogenous cell populations. J Immunol Methods 180:131-140.
Durraffour S, Andrei G, Topalis D, Krecmerova, M, Crance JM, Garin D, Snoeck R. 2012. Mutations conferring resistance to viral DNA polymerase inhibitors in camelpox virus give different drug-susceptibility profiles in vaccinica virus. J Virol 86(13):7310-7325.

Durski KN, McCollum AM, Nakazawa Y, Petersen BW, Reynolds MG, Briand S, Harouna Djingarey M, Olson V, Damon IK, Khalakdina A. 2018. Emergence of

Monkeypox – West and Central Africa, 1970 – 2017. MMWR-Morbid Mortal W 67(10):306-310.

Dyall J, Johnson RF, Chen D, Huzella L, Ragland DR, Mollura DJ, Byrum R, Reba RC, Jennings G, Jahrling PB, Blaney JE, Paragas J. 2011. Evaluation of Monkeypox disease progression by molecular imaging. J Infect Dis 204:1902-1911.

Earl PL, America JL, Wyatt LS, Eller LA, Whitbeck JC, Cohen GH, Eisenberg RJ, Hartmann CJ, Jackson DL, Kulesh DA, Martinez MJ, Miller DM, Mucker EM, Shamblin JD, Swiers SH, Huggins JW, Jahrling PB, Moss B. 2004. Immunogenicity of a highly attenuated MVA smallpox vaccine and protection against monkeypox. Nature 428:182-185.

Engler RJ, Kenner J, Leung DYM. 2002. Smallpox vaccination: Risk considerations for patients with atopic dermatitis. J Allergy Clin Immunol 110:357-365.

Esposito JJ, Fenner F. 2001. Fields Virology. 4th ed. Philadelphia (PA): Lippincott Williams & Wilkins.

European Centre for Disease Prevention and Control (ECDC). [Internet]. [updated 2018 21 Sep]. Monkeypox cases in the UK imported from travelers returning from Nigeria, 2018; [cited 2018 Dec 15]. Available from: https://ecdc.europa.eu/en/publications-data/rapid-risk-assessment-monkeypox-cases-uk-imported-travellers-returning-nigeria

Fantuzzi G, Dinarello CA. 1999. Interleukin-18 and interleukin-1 beta: two cytokine substrates for ICE (caspase-1). J Clin Immunol 19(1):1-11.

Falendysz EA, Lopera JG, Lorenzsonn F, Salzer JS, Hutson CL, Doty J, Gallardo-Romero N, Carroll DS, Osorio JE, Rocke TE. 2015. Further Assessment of Monkeypox Virus Infection in Gambian Pouched Rats (Cricetomys gambianus) Using In Vivo Bioluminescent Imaging. PLoS Negl Trop Dis 9(10):e0004130.

Fang M, Sigal LJ. 2005. Antibodies and CD8+ T cells are complementary and essential for natural resistance to a highly lethal cytopathic virus. J Immunol 175:6829-6836.

Fang M, Lanier LL, Sigal LJ. 2008. A role for NKG2D in NK cell-mediated resistance to poxvirus disease. PLoS Pathog 4(2):e30.

Fenner F, Henderson DA, Arita I, Jezek Z, Ladnyi ID. 1988. Smallpox and its eradication. Switzerland: World Health Organization.

Food and Drug Administration (FDA). 2018. [Internet]. [updated 2018 18 Dec]. Smallpox Preparedness and Response Updates from FDA [cited 2019 Apr 07]. Available from: https://www.fda.gov/EmergencyPreparedness/Counterterrorism/MedicalCountermeasures/MCMIssues/ucm612713.htm.

Foster SA, Parker S, Lanier R. 2017. The role of Brincidofovir in preparation for a potential smallpox outbreak. Viruses 9(11):320.

Fuller VJ, Kolb RW. 1968. Comparison of titrations on the chorioallantoic membrane of chick embryos with the rabbit scarification technique for the potency assay of smallpox vaccines. Appl Microbiol 16(3):458-462.

Fung-Leung WP, Schilham MW, Rahemtulla A, Kundig TM, Vollenweider M, Potter J, van Ewijk W, Mak TW. 1991. CD8 is needed for development of cytotoxic T cells but not helper T cells. Cell 65(3):443-449.

Galluzzi L, Vitale I, Abrams JM, Alnemri ES, Baehrecke EH, Blagosklonny MV, Dawson TM, Dawson DL, El-Deiry WS, Fulda S, Gottliem E, Green DR, Hengartner MO, Kepp O, Knight RA, Kumar S, Lipton SA, Lu X, Madeo F, Malorni W, Mehlen P, Nunez G, Peter ME, Piacentini M, Rubinsztein DC, Shi Y, Simon HU, Vandenabeele P, White E, Yuan J, Zhivotovsky B, Melin G, Kroemer G. Molecular definitions of cell death subroutines: recommendations on the Nomenclature Committee on Cell Death 2012. Cell Death Differ 19(1):107–120.

Grosenbach DW, Honeychurch K, Rose EA, Chinsangaram J, Frimm A, Maiti B, Lovejoy C, Meara I, Long P, Hruby DE. 2018. Oral Tecovirimat for the treatment of smallpox. N Engl J Med 379:44-53.

Hodgman M, Marraffa JM, Wojcik S, Grant W. 2017. Serum calcium concentration in ethylene glycol poisoning. J Med Toxicol 13(2): 153–157.

Hooper JW, Thompson E, Wilhelmsen C, Zimmerman M, Ait Ichou M, Steffen SE, Schmaljohn CS, Schmaljohn AL, Jahrling PB. 2004. Smallpox DNA vaccine protects nonhuman primates against lethal monkeypox. J Virol 78(9):4433-4443.

Huhn GD, Bauer AM, Yorita K, Graham MB, Sejvar J, Likos A, Damon IK, Reynolds MG, Kuehnert MJ. 2005. Clinical characteristics of human monkeypox, and risk factors for severe disease. Clin Infect Dis 41:1742-1751.

Hutin JFY, Williams RJ, Malfait P, Pebody R, Loparev VN, Ropp SL, Rodriguez M, Knight JC, Tshioko FK, Khan AS, Szczeniowski MV, Esposito JJ. 2001. Outbreak of human monkeypox, Democratic Republic of Congo, 1996-1997. Emerg Infect Dis 7(3):434-438.

Hutson CL, Nakazawa YJ, Self J, Olson VA, Regnery RL, Braden Z, Weiss S, Malekani J, Jackson E, Tate M, Karem KL, Rocke TE, Osorio JE, Damon IK, Carroll DS. 2015. Laboratory Investigations of African Pouched Rats (Cricetomys gambianus) as a Potential Reservoir Host Species for Monkeypox Virus. PLoS Negl Trop Dis. 9(10):e0004013.

Jacobs BL, Langland JO, Kibler KV, Denzler KL, White SD, Holecheck SA, Wong S, Huynh T, Baskin CR. 2009. Vaccinia virus vaccines: past, present, and future. Antivir Res 84(1):1-13.

Jahrling PB, Fritz EA, Hensley LE. 2005. Countermeasures to the bioterrorist threat of smallpox. Curr Mol Med 5:817-826.

Jezek Z, Szczeniowski M, Paluko KM, Mutombo M. 1987. Human monkeypox: clinical features of 282 patients. J Infect Dis 156(2):293-298.

Johnson N, Ng TT, Parkin JM. 1997. Camptothecin causes cell cycle perturbations within T-lymphoblastoid cells followed by dose dependent induction of apoptosis. Leuk Res 21(10):961-972.

Johnson RF, Yellayi S, Cann JA, Johnson A, Smith AL, Paragas J, Jahrling PB, Blaney JE. 2011. Cowpox virus infection of cynomolgus macaques as a model of hemorrhagic smallpox. Virology 418:102-112.

Kanegane H, Hoshino A, Okano T, Yasumi T, Wada T, Takada H, Okada S, Yamashita M, Yeh T, Nishikomori R, Takagi M, Imai K, Ochs HD, Morio T. 2017. Flow cytometry-based diagnosis of primary immunodeficiency diseases. Allergol Int 67(1):43-54.

Karupiah G, Buller RM, Van Rooijen N, Duarte CJ, Chen J. 1996. Different roles for CD4+ and CD8+ T lymphocytes and macrophage subsets in the control of a generalized virus infection. J Virol 70:8301–8309.

Kawabe T, Naka T, Yoshida K, Tanaka T, Fujiwara H, Suematsu S, Yoshida N, Kishimoto T, Kikutani H. 1994. The immune responses in CD40-deficient mice: impaired immunoglobulin class switching and germinal center formation. Immunity 1(3):167-178.

Kennedy R, Poland GA. 2007. T-Cell epitope discovery for variola and vaccinia viruses. Rev Med Virol 17: 93–113.

Kitamura D, Roes J, Kuhn R, Rajewsky K. 1991. A B cell-deficient mouse by targeted disruption of the membrane exon of the immunoglobulin mu chain gene. Nature 350:423-426.

Krause JR, Penchansky L, Contis L, Kaplan SS. Flow cytometry in the diagnosis of acute leukemia. Am J Clin Pathol. 1988 89(3):341-6.

Lenardo M. 2017. National Institutes of Health. Laboratory of Immune System Biology. [Internet]. [cited date 2019 Oct 15]. Available from: https://www.niaid.nih.gov/research/michael-j-lenardo-md

Leong TY, Leong AS. 2007. How does antigen retrieval work? Adv Anat Pathol 14(2):129-131.

Leparc-Goffart I, Poirier B, El Zaouk A, Tissier MH, Fuchs F. 2003. New generation of cell culture assay for smallpox vaccine potency. J Clin Microbiol 41(8):3687-3689.

Likos AM, Sammons SA, Olson VA, Frace AM, Li Y, Olsen-Rasmussen M, Davidson W, Galloway R, Khristova ML, Reynolds MG, Zhao H, Carroll DS, Curns A, Formenty P, Esposito JJ, Regnery RL, Damon IK. 2005. A tale of two clades: monkeypox viruses. J Gen Virol 86:2661-2672.

Lippé R. 2018. Flow Virometry: a Powerful Tool To Functionally Characterize Viruses. J Virol 92(3) e01765-17. [Internet]. [cited 17 Oct 2019] Available from https://jvi.asm.org/content/92/3/e01765-17/figures-only?sid=78bb846b-51d8-4280-905e-f4232489c287

Magnus Pv, Andersen EK, Petersen KB, Birch-Andersen A. 1959. A pox-like disease in cynomolgus monkeys. Acta Pathol Mic Sc 46(2):156-176.

Maecker H, Trotter J. 2012. BD Biosciences Application Note: selecting reagents for multicolor flow cytometry [Internet]. [cited 2019 Oct 15]. Available from: http://web.mit.edu/flowcytometry/www/Becton%20Dickinson%20Multicolor_AppNote.pdf

Man S, Karki R, Kanneganti T. 2018. Molecular mechanisms and functions of pyroptosis, inflammatory caspases and inflammasomes in infectious diseases. Immunol Rev 277(1): 61–75.

Marennikova SS, Seluhina EM, Mal'Ceva NN, Cimiskjan KL, Macevic GR. 1972. Isolation and properties of the causal agent of a new variola-like disease (monkeypox) in man. Bull Org mond Sante Bull Wld Hlth Org 46:599-611.

Martin SJ, Reutelingsperger CPM, McGahon AJ, Rader JA, van Schie RCAA, LaFace DM, Green DR. 1995. Early redistribution of plasma membrane phosphatidylserine is a general feature of apoptosis regardless of the initiating stimulus: Inhibition by overexpression of Bcl-2 and Abl. J Exp Med 182:1545-1556.

McConnell S, Herman YF, Mattson DE, Huxsoll DL, Lang CM, Yager RH. 1964. Protection of rhesus monkeys against monkeypox by vaccinica virus immunization. Am J Vet Res 25:192-195.

McFadden G. 2005. Poxvirus tropism. Nat Rev Microbiol 3(3): 201-213.

McIntosh AA, Smith GL. 1996. Vaccinica virus glycoprotein A34R is required for infectivity of extracellular enveloped virus. J Virol 70(1):272-81.

Moriwaki K, Ka-Ming Chan F. 2013. RIP3: a molecular switch for necrosis and inflammation. Genes Dev 27:1640-1649.

Moss B. 2001. Fields Virology. 4th ed. Philadelphia (PA): Lippincott Williams & Wilkins.

Moss B, Shisler JL. 2001. Immunology 101 at poxvirus U: Immune evasion genes. Semin Immunol 13:59-66.

Naesens L, Snoeck R, Andrei G, Balzarini J, Neyts J, De Clercq E. 1996. HPMPC (cidofovir), PMEA (adefovir) and related acyclic nucleoside phosphonate analogues: a review of their pharmacology and clinical potential in the treatment of viral infections. Antivir Chem Chemother 8(1):1-23.

Nakazawa Y, Emerson GL, Carroll DS, Zhao H, Li Y, Reynolds MG, Karem KL, Olson VA, Lash RR, Davidson WB, Smith SK, Levine RS, Regnery RL, Sammons SA, Frace MA, Elmango MM, Karsani MEM, Muntasir MO, Babiker AA, Opoka L, Chowdhary V, Damon IK. 2013a. Phylogenetic and ecological perspectives of a Monkeypox outbreak, southern Sudan, 2005. Emerg Infect Dis 19(2): 237–245.

Nakazawa Y, Lash RR, Carroll DS, Damon IK, Karem KL, Reynolds MG, Osorio JE, Rocke TE, Malekani JM, Muyembe JJ, Formenty P, Peterson AT. 2013b. Mapping Monkeypox transmission risk through time and space in the Congo Basin. PLoS ONE 8(9):e74816.

Nalca A, Rimoin AW, Bavari S, Whitehouse CA. 2005. Reemergence of monkeypox: prevalence, diagnostics, and countermeasures. Clin Infect Dis 41:1765-1771.

National Institutes of Health Clinical Center (NIH CC). [Internet]. [updated 2008 04 Mar]. Phase I/II trial of Modified Vaccinia Virus Ankara (MVA) vaccine against Smallpox; [cited 2019 Apr 07]. Available from: https://clinicaltrials.gov/ct2/show/study/NCT00053742#wrapper

Negroni A, Cucchiara S, Stronati L. 2015. Apoptosis, necrosis, and necroptosis in the gut and intestinal homeostasis [Internet]. [accessed 12 October 2019]. Mediators of Inflammation 2015(2). Available from: https://www.researchgate.net/publication/283674912_Apoptosis_Necrosis_and_Necroptosis_in_the_Gut_and_Intestinal_Homeostasis

NIH Nonhuman Primate Reagent Resource. 2004. Reagents by Species [Internet]. [cited 2010 May 13]. Available from: https://www.nhpreagents.org/NHP/ReagentBySpecies.aspx?Species=9

Noelle RJ, Roy M, Shepherd DM, Stamenkovic I, Ledbetter JA, Aruffo A. 1992. A 39-kDa protein on activated helper T cells binds CD40 and transduces the signal for cognate activation of B cells. Proc. Natl. Acad. Sci. USA 89:6550–6554.

O'Neil-Anderson NJ, Lawrence DA. 2002. Differential modulation of surface and intracellular protein expression by T cells after stimulation in the presence of Monensin or Brefeldin A. Clin Diagn Lab Immunol 9(2): 243–250.

Owen JA, Punt J, Stranford SA, Jones PP. 2013. Kuby Immunology. 7th ed. New York (NY): W.H. Freeman and Company.

Parker N, Schneegurt M, Thi Tu A, Lister P, Forster BM, Allen S, Auman A, Brelles-Marino G, Feldman MA, Flowers P, Pinchuk G, Rowley B, Sutherland M, Franklund C, Paterson A. 2016. Microbiology [Internet]. Sterling (VA): OpenStax CNX and the American Society for Microbiology Press; [cited 06 October 2019]. Available from: http://cnx.org/contents/e42bd376-624b-4c0f-972f-e0c57998e765@4.2

Paul WE (Editor). 2013. Fundamental Immunology. 7th ed. Philadelphia (PA): Lippincott Williams & Wilkins

Petersen BW, Damon IK, Pertowski CA, Meaney-Delman D, Guarnizo JT, Beigi RH, Edwards KM, Fisher MC, Frey SE, Lynfield R, Willoughby RE. 2015. Clinical guidance for smallpox vaccine use in a postevent vaccination progr`am. MMWR Recomm Rep 64(RR-02):1-26.

Petersen CM, Christensen EI, Andresen BS, Møller BK. 1992. Internalization, lysosomal degradation and new synthesis of surface membrane CD4 in phorbol ester-activated T-lymphocytes and U-937 cells. Exp Cell Res 201(1):160-173.

Promega Corporation. 2019. Real-Time Monitoring of Apoptosis Progression. [Internet]. [cited 3 Oct 2019] Available from https://promega.media/-/media/images/resources/articles-and-publications/pubhub/featured-articles/annexin-v-feature/annexinv-apoptosis-detection-1200x1200.jpg

Poland GA, Grabenstein JD, Neff JM. 2005. The US smallpox vaccination program: a review of a large modern era smallpox vaccination implementation program. Vaccine 23: 2078-2081.

Reed KD, Melski JW, Graham MB, Regnery RL, Sotir MJ, Wegner MV, Kazmierczak, Stratman EJ, Li Y, Fairley JA, Swain GR, Olson VA.Sargent EK, Kehl SC, Frace MA, Kline R, Foldy SL, David JP, Damon IK. 2004. The Detection of Monkeypox in Humans in the Western Hemisphere. N Engl J Med 350:342-350.

Renshaw BR, Fanslow WC 3rd, Armitage RJ, Campbell KA, Liggitt D, Wright B, Davison BL, Maliszewski CR. Humoral immune responses in CD40 ligand-deficient mice. J Exp Med 180(5):1889-1900.

Ruegg CL, Rajasekar S, Stein BS, Engleman EG. 1992. Degradation of CD4 following phorbol induced internalization in human T lymphocytes. Evidence for distinct endocytic routing of CD4 and CD3. J Biol Chem 267(26):18837-18843.

Saijo M, Ami Y, Suzaki Y, Nagata N, Hasegawa H, Iizuka I, Shiota T, Sakai K, Ogata M, Fukushi S, Mizutani T, Sata T, Kurata T, Kurane I, Morikawa S. 2009. Virulence and pathophysiology of the Congo Basin and West African strains of monkeypox virus in non-human primates. J Gen Virol 90(Pt 9):2266-2271.

Seet BT, Johnston JB, Brunetti CR, Barrett JW, Everett H, Cameron C, Sypula J, Nazarian SH, Lucas A, McFadden G. 2003. Poxviruses and immune evasion. Annu Rev Immunol 21:377-423.

Shchelkunov SN, Totmenin AV, Safronov PF, Mikheev MV, Gutorov VV, Ryazankina OI, Petrov NA, Babkin IV, Uvarova EA, Sandakhchiev LS, Sisler JR, Esposito JJ, Damon IK, Jahrling PB, Moss B. 2002. Analysis of the monkeypox virus genome. Virology. 297:172-194.

Slee EA, Adrain C, Martin SJ. 2001. Executioner caspase-3, -6, and -7 perform distinct, non-redundant roles during the demolition phase of apoptosis. J Biol Chem 276(10):7320-7326.

Smee DF, Bailey KW, Sidwell RW. 2001. Treatment of lethal vaccinia virus respiratory infections in mice with cidofovir. Antivir Chem Chemother 12:71-76.

Smee DF, Bailey KW, Wong MH, Sidwell RW. 2000. Intranasal treatment of cowpox virus respiratory infections in mice with cidofovir. Antivir Res 47:171-177.

Smee DF, Sidwell RW. 2003. A review of compounds exhibiting anti-orthopoxvirus activity in animal models. Antivir Res 57:41-52.

Song H, Janosko K, Johnson RF, Qin J, Josleyn N, Jett C, Byrum R, St. Claire M, Dyall J, Blaney JE, Jennings G, Jahrling PB. 2013. Poxvirus antigen staining of immune cells as a biomarker to predict disease outcome in Monkeypox and Cowpox Virus infection in non-human primates. PLoS ONE 8(4):e60533.

Tait JF, Gibson D. 1994. Measurement of membrane phospholipid asymmetry in normal and sickle-cell erythrocytes by means of annexin V binding. Lab Clin Med 123(5):741-8.
Upton JW, Ka-Ming Chan F. 2014. Staying alive: Cell death in anti-viral immunity. Mol Cell 54(2): 273-280.

ThermoFisher Scientific. 2019. Best protocols: viability staining protocol for flow cytometry.
[cited 2019 Oct 16]. Available from:
https://www.thermofisher.com/us/en/home/references/protocols/cell-and-tissue-analysis/protocols/viability-staining-flow-cytometry.html

Vanlangenakker N, Vanden Berghe T, Vandenabeele P. 2012. Many stimuli pull the necrotic trigger, an overview. Cell Death Differ 19:75–86.

Wahl-Jensen V, Cann JA, Rubins KH, Huggins JW, Fisher RW, Johnson AJ, de Kok-Mercado F, Larsen T, Raymond JL, Hensley LE, Jahrling PB. 2011. Progression of pathogenic events in cynomolgus macaques infected with variola virus. PLoS One 6(10):e24832.

Weir EG, Borowitz MJ. 2002. Flow cytometry in the diagnosis of acute leukemia. Semin Hematol 38(2):124-38.

Wlodkowic D, Telford W, Skommer J, Darzynkiewicz Z. 2011. Apoptosis and beyond: cytometry in studies of programmed cell death. Methods Cell Biol 103: 55–98.

Wlodkowic D, Skommer J, Darzynkiewicz Z. 2012. Cytometry of apoptosis. Historical perspective and new advances. Exp Oncol 34(3): 255-262.

World Health Organization (WHO) [Internet]. [updated 2018 5 Oct]. Emergencies preparedness, response Monkeypox – Nigeria; [cited 2018 Oct 11]. Available from: https://www.who.int/csr/don/05-october-2018-monkeypox-nigeria/en/

World Health Organization (WHO). 1999. Technical advisory group on human Monkeypox: a report of a WHO meeting, Geneva, Switzerland, 11-12 January 1999. WHO/CDS/CSR/APH/99.5.

Xu RH, Cohen M, Tang Y, Lazear E, Whitbeck JC, Eisenberg RJ, Cohen GH, Sigal LJ. 2008. The orthopoxvirus type I IFN binding protein is essential for virulence and an effective target for vaccination. J Exp Med 205(4):981-992.

Zaucha GM, Jahrling PB, Geisberg TW, Swearengen JR, Hensley L. 2001. The pathology of experimental aerosolized Monkeypox virus infection in cynomolgus monkeys (*Macaca fascicularis)*. Lab Invest 81(12):1581-1600.